Polo-like kinase phosphorylation of bilobe-resident TbCentrin2 facilitates flagellar inheritance in *Trypanosoma brucei*

Christopher L. de Graffenried[a], Dorothea Anrather[b], Freia Von Raußendorf[c], and Graham Warren[a,c]

[a]Max F. Perutz Laboratories, Center for Molecular Biology, University of Vienna, 1030 Vienna, Austria; [b]Max F. Perutz Laboratories, Department of Biochemistry, Mass Spectrometry Facility, University of Vienna, 1030 Vienna, Austria; [c]Max F. Perutz Laboratories, Department of Medical Biochemistry, Medical University of Vienna, 1030 Vienna, Austria

ABSTRACT **In the protist parasite *Trypanosoma brucei*, the single Polo-like kinase (TbPLK) controls the inheritance of a suite of organelles that help position the parasite's single flagellum. These include the basal bodies, the bilobe, and the flagellar attachment zone (FAZ). TbCentrin2 was previously shown to be a target for TbPLK in vitro, and this is extended in this study to in vivo studies, highlighting a crucial role for serine 54 in the N-terminal domain. Duplication of the bilobe correlates with the presence of TbPLK and phospho-TbCentrin2, identified using phosphospecific antiserum. Mutation of S54 leads to slow growth (S54A) or no growth (S54D), the latter suggesting that dephosphorylation is needed to complete bilobe duplication and subsequent downstream events necessary for flagellum inheritance.**

Monitoring Editor
Francis A. Barr
University of Oxford

Received: Dec 31, 2012
Revised: Mar 26, 2013
Accepted: Apr 16, 2013

INTRODUCTION

Trypanosoma brucei is a flagellated protist parasite that causes African sleeping sickness in humans and nagana in cattle. *T. brucei* is an obligate extracellular pathogen that relies on its motility for immune evasion and dissemination in mammals and for transit from the midgut to the salivary glands of its insect host (Hill, 2010). The parasite's motility is generated by a single flagellum that is nucleated at the posterior of the cell by the basal body and emerges from an invagination of the cell surface known as the flagellar pocket (Field and Carrington, 2009; Lacomble *et al.*, 2009). Once outside the cell, the flagellum adheres along the length of the cell body and extends approximately 2 μm beyond the end of the cell. The placement of the flagellum within the flagellar pocket and its adherence to the cell body are essential for the motility of *T. brucei* (LaCount *et al.*, 2002; Bonhivers *et al.*, 2008; Vaughan *et al.*, 2008). This positional information must be duplicated and inherited along with the flagellum during cell division.

Several cytoskeletal organelles are responsible for positioning and adhering the flagellum to the cell surface. Near the top of the flagellar pocket, an electron-dense annulus known as the flagellar pocket collar forms a seal between the flagellar membrane and the cell surface (Sherwin and Gull, 1989; Bonhivers *et al.*, 2008). A structure known as the bilobe is present at the top of the flagellar pocket and extends toward the anterior of the cell (Esson *et al.*, 2012; Gheiratmand *et al.*, 2013). The bilobe was originally implicated in Golgi duplication and is composed of two distinct arms marked by TbCentrin4 and TbMORN1 (He *et al.*, 2005; Selvapandiyan *et al.*, 2007; Shi *et al.*, 2008; Morriswood *et al.*, 2009). A bead-like filament known as the flagellum attachment zone (FAZ) begins between the two arms of the bilobe and extends toward the anterior end of the cell (Vickerman, 1969; Gull, 1999). The FAZ traverses the plasma membrane and contacts the flagellum, keeping it tightly held to the cell surface along the whole length of the cell. A set of four microtubules, known as the microtubule quartet, nucleate at the basal body, wrap around the flagellar pocket, and then run beside the FAZ filament. These cytoskeletal elements are depicted in Supplemental

This article was published online ahead of print in MBoC in Press (http://www.molbiolcell.org/cgi/doi/10.1091/mbc.E12-12-0911) on April 24, 2013.

Address correspondence to: Christopher L. de Graffenried (Christopher_degraffenried@brown.edu)

Abbreviations used: CIP, calf intestinal alkaline phosphatase; DIC, differential interference contrast; FAZ, flagellum attachment zone.

Figure S1. Depletion of the molecular components of these structures causes defects in flagellar pocket duplication and flagellar adherence (LaCount *et al.*, 2002; Selvapandiyan *et al.*, 2007; Bonhivers *et al.*, 2008; Vaughan *et al.*, 2008).

During cell division, the flagellum must be duplicated and positioned within the daughter cell. This process begins with the maturation of the probasal body, which nucleates a new flagellum that inserts into the flagellar pocket (Sherwin and Gull, 1989; Lacomble *et al.*, 2010). The new flagellum extends until it emerges at the cell surface, at which point it has been incorporated into its own flagellar pocket (Gadelha *et al.*, 2009; Lacomble *et al.*, 2010). The assembly of a new FAZ then begins; its construction trails slightly behind the elongation of the flagellum, adhering it to the cell surface (Kohl *et al.*, 1999). The assembly of the new bilobe and FAZ must occur at specific points during the extension of the new flagellum to ensure that it incorporates into its own flagellar pocket and is attached to the cell surface, indicating that the assembly of the new flagellum and the organelles that position it is coordinated.

We have recently shown that the duplication of the bilobe and FAZ require the single Polo-like kinase homologue in *T. brucei*, known as TbPLK (de Graffenried *et al.*, 2008; Ikeda and de Graffenried, 2012). The kinase migrates from the posterior to the anterior of the cell during the cell cycle and is present on the basal body, bilobe, and FAZ as the structures are duplicating. Depleting TbPLK causes defects in the inheritance of these three structures, leading to cells that have basal body segregation defects, deformed bilobes, and FAZ defects; these cells cannot undergo cytokinesis (Ikeda and de Graffenried, 2012). While new flagellar assembly is not impaired, TbPLK depletion makes it impossible for cells to place flagella in the necessary context to function properly. The substrates that TbPLK phosphorylates are currently unknown; most of the established PLK substrates present in mammalian cells, such as cdc25 and Bub1, appear to be absent in *T. brucei* (Li *et al.*, 2010; Szöör, 2010).

Recently the centrin homologue TbCentrin2 was identified as an in vitro TbPLK substrate (de Graffenried *et al.*, 2008; Yu *et al.*, 2012). Centrins are highly conserved calcium-binding proteins that are components of microtubule-organizing centers and the contractile fibers associated with them (Salisbury, 1995). Centrins are usually composed of two pairs of calcium-binding EF-hand domains separated by an alpha helix, giving the protein a barbell-like shape (Sheehan *et al.*, 2006; Thompson *et al.*, 2006). While centrins appear to be involved in many cellular processes, their precise function is not well understood. They are rapidly phosphorylated in response to environmental cues, such as pH shock in green algae and light in mammalian photoreceptor cells (Salisbury *et al.*, 1984; Martindale and Salisbury, 1990; Trojan *et al.*, 2008). Centrins are also phosphorylated during cell division, and this modification plays a role in centriole duplication and separation (Lutz *et al.*, 2001; Araki *et al.*, 2010; Yang *et al.*, 2010).

TbCentrin2 localizes to the basal body, bilobe, and flagellum in *T. brucei*, making it possible that TbCentrin2 encounters TbPLK during the cell cycle (He *et al.*, 2005; Wang *et al.*, 2012; Bangs, 2011). In this article, we have mapped the phosphosites present on TbCentrin2 in vivo and those generated by TbPLK in vitro using mass spectrometry. We identified Ser-54, which is phosphorylated in vitro and in vivo, and generated a phosphospecific antiserum that detects this site. Immunofluorescence showed that the TbCentrin2 present on the bilobe is phosphorylated at Ser-54 as the bilobe duplicates, which also correlates with the presence of TbPLK on this structure. Using a complemented conditional knockout system, we show that mutation of Ser-54 causes defects in the assembly of the bilobe and FAZ, which leads to detached flagella and defects in cytokinesis. Phosphorylation of TbCentrin2 at Ser-54 by TbPLK is an important event in the cell cycle that plays a role in the assembly of a new bilobe and FAZ.

RESULTS

A monoclonal antibody specific for TbCentrin2 labels the basal body, flagellum, and bilobe structure

In trypanosomes, TbCentrin2 has been shown to localize predominantly to the bilobe and basal bodies, with some labeling also present on the flagellum (He *et al.*, 2005; Morriswood *et al.*, 2009). However, the localization of TbCentrin2 has relied on the monoclonal antibody 20H5 and a rabbit polyclonal antibody raised against whole TbCentrin2 for detection (Wang *et al.*, 2012). Originally raised against *Chlamydomonas* centrin, 20H5 detects a host of centrins in different organisms (Sanders and Salisbury, 1994; Klotz *et al.*, 1997; He *et al.*, 2005). We therefore sought to generate a specific monoclonal antibody that exclusively detects TbCentrin2. During a screen of hybridomas generated from mice injected with recombinant TbCentrin2, we identified a monoclonal that we termed 2B2H1, which appeared selective for this centrin. To determine the basis for this specificity, we identified the binding epitope of the antibody by truncating TbCentrin2 and testing the fragments for 2B2H1 reactivity using Western blotting (Figure S2). The TbCentrin2 truncations were appended to the maltose-binding protein tagged with a His_{10} tag, expressed in *Escherichia coli*, and purified by nickel chromatography under denaturing conditions. By continuously shortening the 2B2H1-reactive fragments, we were able to show that the antibody epitope falls within a 10–amino acid sequence in the N-terminus of TbCentrin2. The N-terminus is one of the few places where centrins vary, with some containing unique extensions prior to the first EF hand (Friedberg, 2006). The sequence that 2B2H1 recognizes (PVAQSVNRSI) is part of the N-terminal extension unique to TbCentrin2. To confirm the specificity of the antibody in vivo, we deleted the N-terminal extension (amino acids 2–33) of TbCentrin2 in cells, using a complemented conditional knockout system (described fully later in the text). Cells lacking the N-terminal extension had no detectable 2B2H1 immunofluorescent signal (Figure S3).

Once the specificity of 2B2H1 had been established, the localization of TbCentrin2 was evaluated at different cell cycle stages. Cells were fixed using methanol and labeled with 2B2H1 and antibodies against *Leishmania donovani* Centrin4, which cross-reacts with TbCentrin4 and is present on the bilobe structure and basal bodies (Figure 1A; Selvapandiyan *et al.*, 2001, 2007). In an asynchronous culture, ~80% of cells have one nucleus and one kinetoplast (1N1K), which contains the mitochondrial DNA in trypanosomes and is attached to the basal body (Robinson and Gull, 1991). The kinetoplast duplicates first, producing cells with one nucleus and two kinetoplasts (1N2K); this is followed by karyokinesis, yielding a cell with two nuclei and two kinetoplasts (2N2K). In cells directly fixed in methanol, TbCentrin2 localized predominantly to the basal body (including the probasal body) and the flagellum at all cell cycle stages, with some cytoplasmic labeling. This cytoplasmic labeling could obscure other weak labeling patterns, so to limit this possibility and to increase antigen accessibility, we extracted cells with detergent prior to methanol fixation to expose the cytoskeleton (Figure 1B). In these preparations, TbCentrin2 clearly appeared on the bilobe, suggesting that the protein is present on the structure. The bilobe is made up of two distinct arms, only one of which contains high levels of TbCentrin4. The lack of total colocalization between TbCentrin2 and TbCentrin4 suggests that TbCentrin2 may also be present on the MORN1-arm of the bilobe or one of the other recently defined subdomains of the structure (Morriswood *et al.*, 2013).

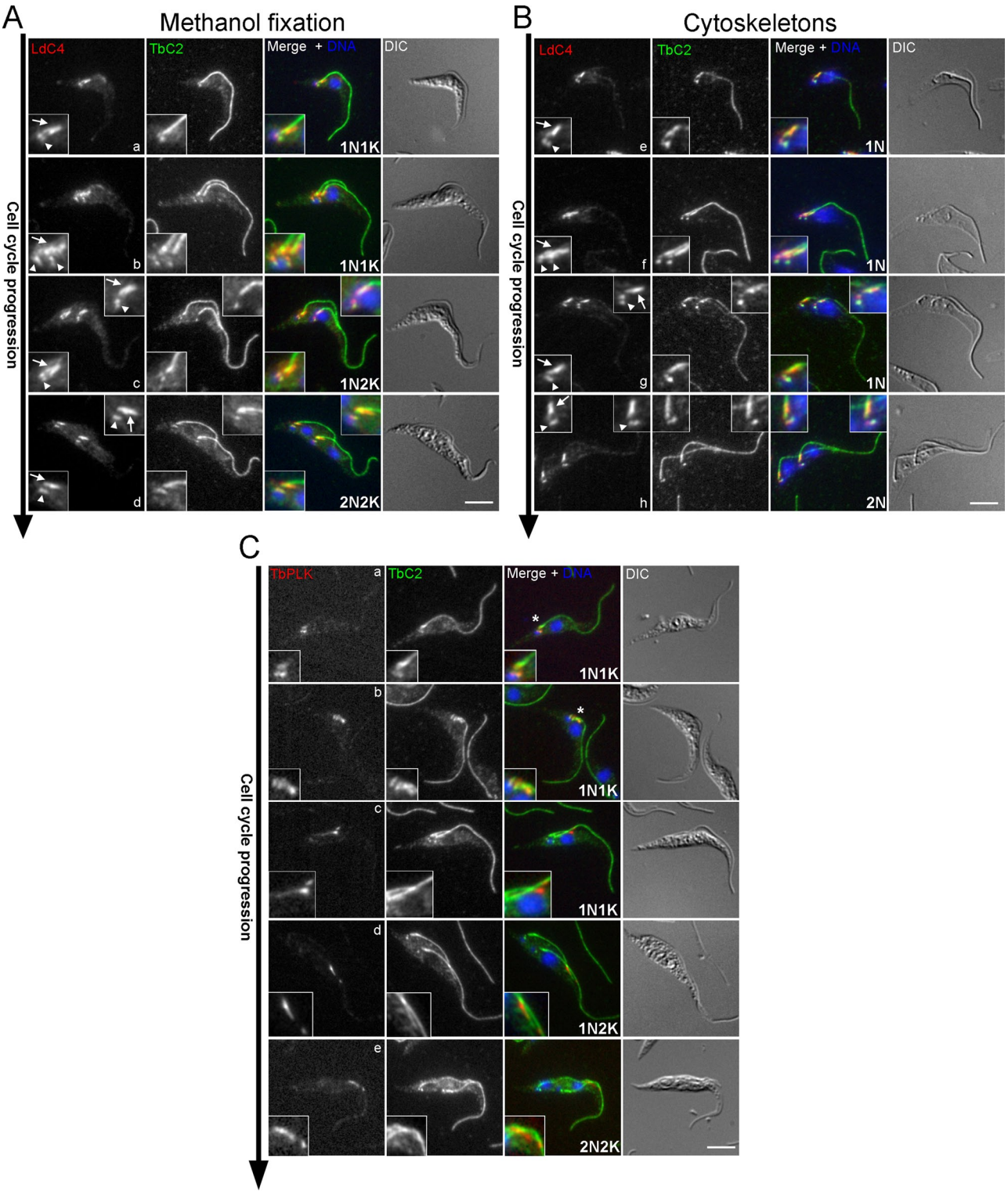

FIGURE 1: TbCentrin2 localizes to the basal body, flagellum, and bilobe. (A) Methanol-fixed cells were stained with anti-LdCentrin4 antibodies (LdC4; red), anti-TbCentrin2, (TbC2; green), and DAPI (DNA; blue) and imaged by fluorescence and DIC microscopy. (B) Cytoskeletons from extracted cells were stained and imaged as in (A). For (A) and (B) the bilobe structure is marked with an arrow and the basal body with an arrowhead; the boxed areas represent 2× magnifications of the bilobe region of each cell. (C) Methanol-fixed cells were stained with anti-TbPLK (TbPLK; red), anti-TbCentrin2 (TbC2; green), and DAPI (DNA; blue) and imaged as in (A). The asterisks mark points where TbPLK and TbCentrin2 partially colocalize. xNyK refers to the number of nuclei (x) and number of kinetoplasts (y) in each cell. Scale bars: 5 μm.

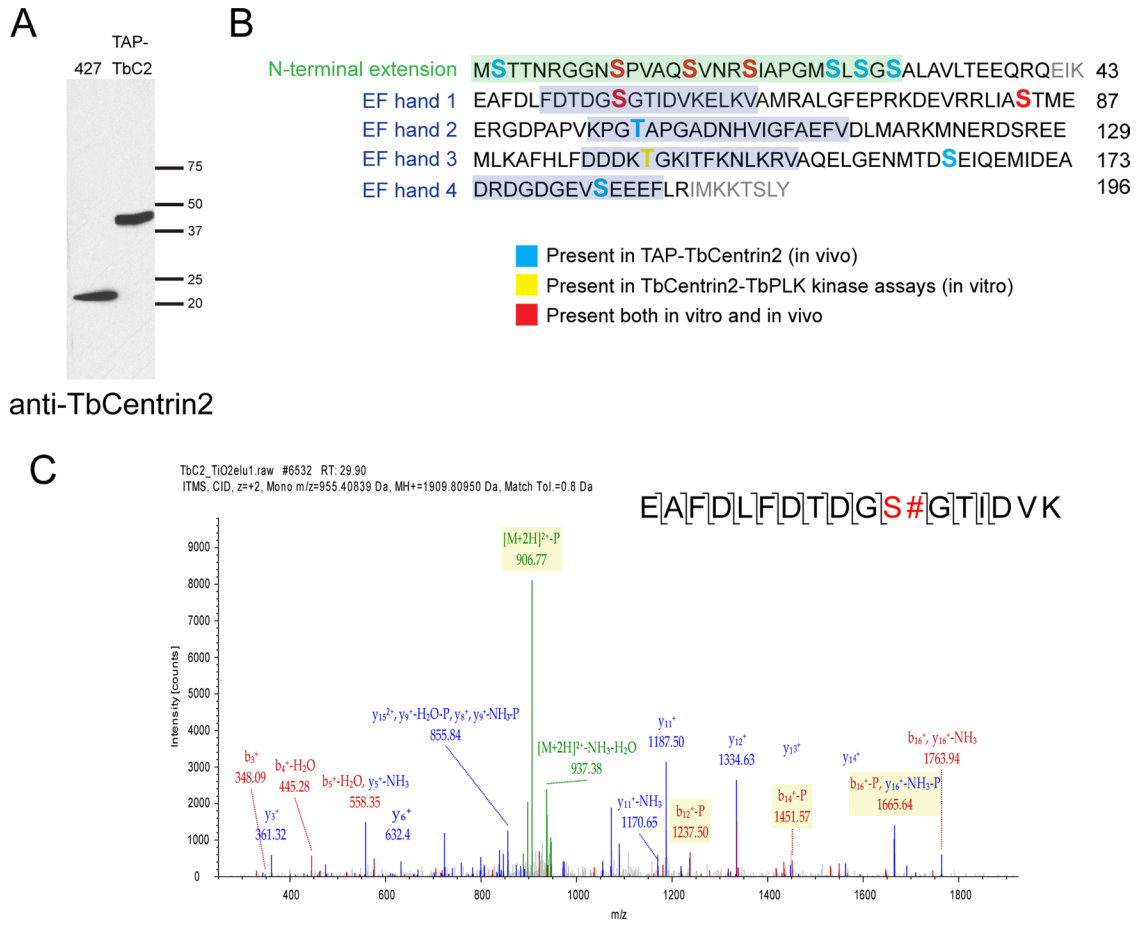

FIGURE 2: TbCentrin2 is phosphorylated at multiple sites in vivo and vitro. (A) Lysates from the parental cell line (427) and the TAP-TbCentrin2 cell line (TAP-TbC2) were probed with anti-TbCentrin2. (B) The TbCentrin2 phosphorylation sites identified in vivo and in vitro. Phosphorylated residues identified exclusively in vivo are shown in blue, and those seen exclusively in vitro are shown yellow, while the sites identified both in vivo and in vitro are shown in red. The N-terminal extension and the EF hands are shaded. The gray text shows the portions of the protein that were not covered by our LC-MS/MS analysis. (C) MS/MS spectrum of an S54 phosphopeptide isolated from purified TAP-TbCentrin2 after TiO_2 enrichment. Identified fragmentations are depicted by lines between amino acids, and S54 is marked in red and with a number symbol.

Cells were fixed in methanol and stained with antibodies against TbPLK and 2B2H1 to identify the points during the cell cycle when the two proteins were on the same structure (Figure 1C). At early stages of the cell cycle, TbPLK is present on the basal bodies and the bilobe structure. Partial colocalization of TbCentrin2 with TbPLK was seen at these stages (Figure 1C, a and b, asterisks), but not later, once the kinase had migrated onto the tip of the new FAZ.

TbCentrin2 is phosphorylated on multiple residues in vivo and a subset of the phosphosites can be generated by TbPLK in vitro

We have previously shown that TbCentrin2 is an in vitro substrate of TbPLK (de Graffenried *et al.*, 2008). To expand upon this work, we sought to identify the phosphosites present on TbCentrin2 in vivo and to catalogue the sites that could be generated on TbCentrin2 by in vitro kinase assays conducted with recombinant TbPLK. The sites present both in vivo and in vitro would be potential TbPLK phosphosites to be investigated further. We endogenously tagged TbCentrin2 with a tandem affinity purification (TAP)-tag at its N-terminus and removed the other allele to show that the tagged copy was functional (Figure 2A). TAP-TbCentrin2 had the same localization pattern as the wild-type protein and the tagged cell line grew at the same rate as the parental line (unpublished data). TAP-TbCentrin2 was purified by two-step TAP purification and subjected to mass spectrometry analysis to identify phosphorylation sites (Figure 2B). Tryptic digests of TbCentrin2 yielded greater than 80% coverage. It is likely that phosphosites generated by TbPLK would be present at low levels, because they are present only during certain points of the cell cycle. To increase yields, we used titanium oxide to enrich the phosphopeptides present in the TAP-TbCentrin2 purifications prior to mass spectrometry (Thingholm *et al.*, 2006). The combined methods identified 12 total phosphosites on TbCentrin2, seven of which were present on the N-terminal extension. Phosphorylation at Ser-10 has previously been identified in a phosphoproteomic screen of bloodstream-form trypanosomes (Nett *et al.*, 2009b). EF hands 1, 2, and 3 all contained a phosphosite.

Once the in vivo phosphosites present on TbCentrin2 were identified, the sites that could be generated by TbPLK in vitro were identified by conducting kinase assays and mapping the phosphorylated products. TbPLK and its kinase-dead mutant were produced in baculovirus-infected insect cells, while TbCentrin2 was expressed in *E. coli*. Kinase assays were conducted using both the wild-type and

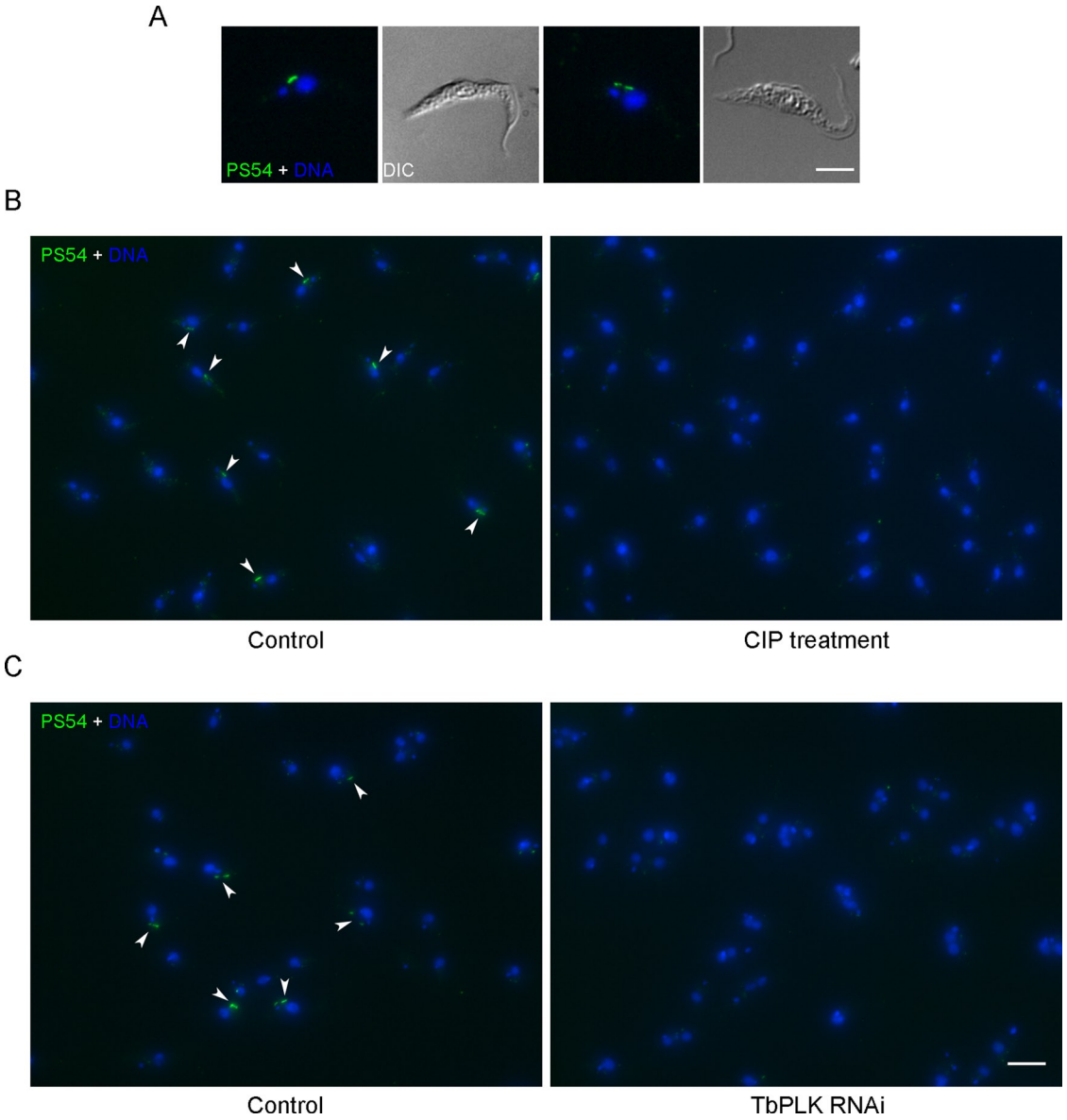

FIGURE 3: PS54 antiserum labels a bar-like structure between the kinetoplast and nucleus in a subset of cells. Cells were fixed in methanol and stained with PS54 (PS54; green) and DAPI (DNA; blue). (A) Note the bar-like structure labeled by PS54. (B) Methanol-fixed cells were incubated overnight in CIP buffer (Control) or CIP buffer containing calf intestinal alkaline phosphatase (CIP treatment) and then stained as in (A). (C) TbPLK RNAi cells were treated for 24 h with vehicle control (Control) or doxycycline to induce RNAi against TbPLK (TbPLK RNAi) before methanol fixation and staining as in (A). Arrowheads in (B) and (C) identify PS54-positive cells. Scale bars: 5 μm (A); 10 μm (B and C).

the kinase-dead mutant of TbPLK. The TbCentrin2 from these assays was subjected to mass spectrometry analysis. No phosphorylation was evident on TbCentrin2 when the kinase-dead mutant of TbPLK was used, while six sites were identified with the wild-type kinase (Figure 2B). All of the sites, except for T142, were present in the in vivo TAP-TbCentrin2 sample, making S10, S15, S19, S54, and S84 potential in vivo TbPLK phosphosites. The MS/MS spectra for S54 is shown in Figure 2C, while the rest of the in vivo sites are shown in Figure S4.

A phosphospecific antiserum against TbCentrin2 S54 labels the bilobe structure during its duplication

On further examination of the TbPLK phosphosites, we chose to focus on S54 (Figure 2C). While there are several phosphosites present in the N-terminal extension of TbCentrin2, previous work on Cdc31p, the yeast centrin homologue, has shown that its N-terminus can be removed without any deleterious effects on growth (Li *et al.*, 2006). We therefore chose to focus initially on phosphosites present in more conserved portions of the protein. We attempted to identify when and where the S54 phosphosite is generated during the cell cycle by employing phosphospecific antiserum raised against the sequence surrounding S54. The phosphopeptide FDTDG(S)GTIDVKELC was conjugated to keyhole limpet hemocyanin and used to immunize rabbits, whose serum was then affinity-purified using the phosphopeptide and absorbed against the unphosphorylated peptide to generate a phosphospecific antiserum that we termed PS54. When used at low dilutions (0.1 μg/ml or lower), the antiserum showed a remarkable specificity for a bar-like structure positioned between the nucleus and kinetoplast in a subset of 1N1K cells (Figure 3A). This signal could be eliminated by

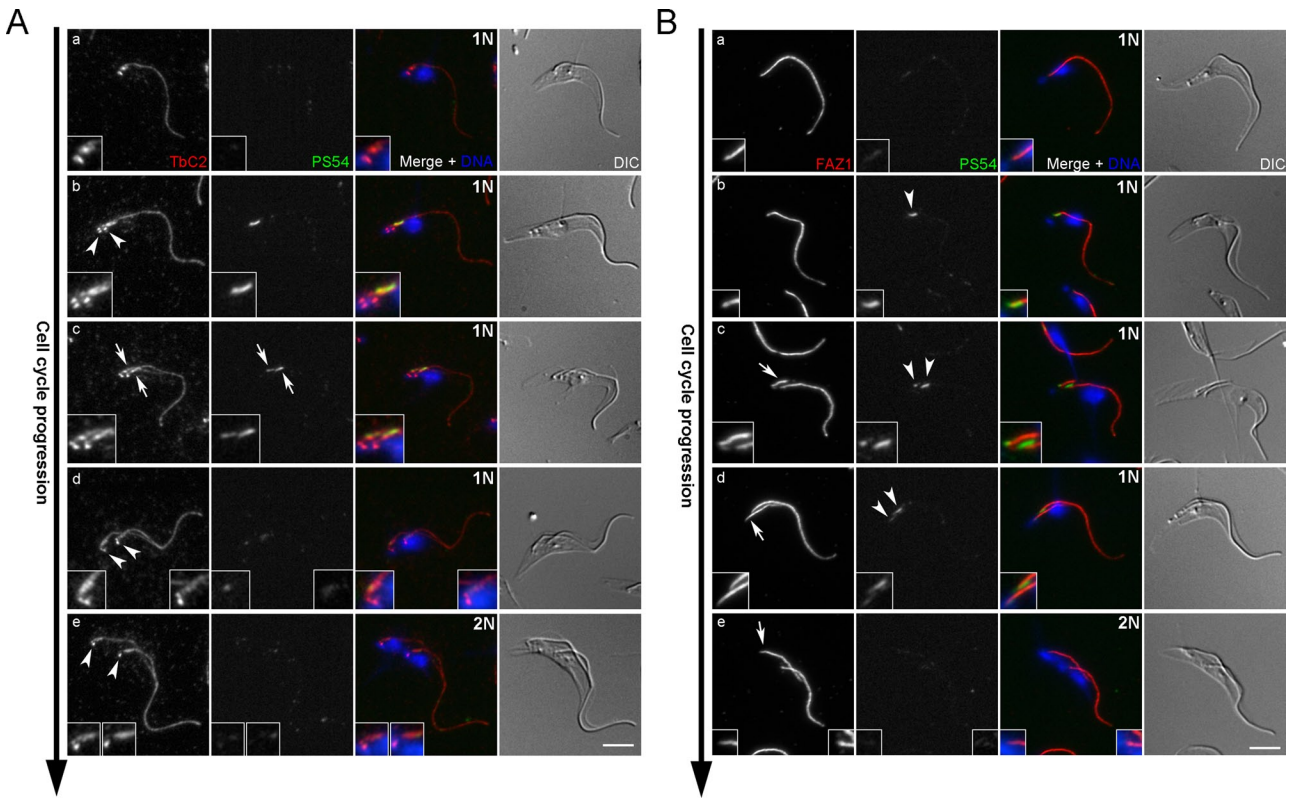

FIGURE 4: The PS54 antiserum labels the bilobe as the structure is duplicating. (A) Cytoskeletons from extracted cells were labeled with anti-TbCentrin2 (TbC2; red), PS54 (PS54; green), and DAPI (DNA; blue) and imaged by fluorescence and DIC microscopy. The inserts show a twofold magnification of the bilobe region of each cell. Most 1N cells are not labeled by PS54 (a), but shortly after basal body duplication (b, arrowheads), PS54 labeling of the bilobe structure became apparent. This labeling persisted during bilobe duplication (c, arrows), but quickly disappeared once the basal bodies began to segregate (d and e, arrowheads). (B) The cytoskeleton was labeled with anti-FAZ1 (FAZ1; red), PS54 (PS54; green), and DAPI (DNA; blue). Initially, the posterior tip of the old FAZ became PS54-positive (b, arrowhead); this was followed by the appearance of a new PS54-positive structure slightly to the posterior of the cell (c, arrowheads), which marks the posterior tip of the new FAZ (c, d, and e, arrow). The PS54 signal rapidly declined once the new FAZ began to elongate (d and e, arrowheads). Scale bars: 5 μm.

incubating the cells with calf intestinal alkaline phosphatase (CIP) prior to labeling with PS54, indicating the antiserum is phosphospecific (Figure 3B). Depletion of TbPLK by RNA interference (RNAi) substantially reduced the PS54 signal (Figure 3C). The PS54 antiserum did not, unfortunately, give any signal by Western blotting when used in the range in which it appears to be phosphospecific.

The position of the PS54-positive structure is very similar to the location of the bilobe structure. For confirmation of this localization, extracted cytoskeletons were labeled with PS54 and the TbCentrin2 monoclonal antibody (Figure 4A). The PS54 antiserum strongly labeled a subset of 1N1K cells with one bilobe or with duplicated bilobes that were still close together. The PS54 signal dropped significantly once basal body segregation began, which appears to drive the separation of the bilobes. Weak labeling could occasionally be seen in 1N2K cells, and essentially no labeling was seen in 2N2K cells. This pattern is consistent with S54 phosphorylation taking place during bilobe duplication, which occurs in 1N1K cells, and being followed by removal of the signal once the duplicated structures begin to separate after kinetoplast separation (Sherwin and Gull, 1989; Ikeda and de Graffenried, 2012).

Cells were stained with PS54 and an antibody against FAZ1, a component of the FAZ filament, to determine the relationship between PS54 phosphorylation and FAZ formation (Figure 4B; Vaughan *et al.*, 2008). The PS54-positive structure appeared in cells with a single FAZ, appearing just above the posterior tip of the filament. This arrangement is similar to what is seen in cells simultaneously labeled for bilobe and FAZ components (Morriswood *et al.*, 2009; Portman and Gull, 2012). A second PS54 positive structure, consistent with the new bilobe, appeared next to the old structure in cells in which the new FAZ filament had begun to form. The PS54 labeling declined on both the old and new structures after kinetoplast duplication and further extension of the new FAZ.

Cells were labeled with a rat monoclonal antibody against TbPLK and PS54 to ascertain how closely expression of the kinase correlated with the appearance of S54 phosphorylation (Figure 5). TbPLK is first seen on the new microtubule quartet, then migrates to the basal body and bilobe as they begin to duplicate (Ikeda and de Graffenried, 2012). PS54 labeling occurred only in TbPLK-expressing cells and was strongest when the kinase was present on the bilobe. The PS54 signal began to diminish after TbPLK had migrated further toward the anterior of the cell along the new FAZ, which occurs as the duplicated bilobes begin to separate.

Mutation of TbCentrin2 S54 causes growth defects

We used complemented conditional knockouts to test the effect of mutating S54 in procyclic cells (Figure S5; Estévez *et al.*, 1999). Briefly, a doxycycline-inducible, Ty1-tagged copy of TbCentrin2 was integrated into cells; this was followed by removal of one

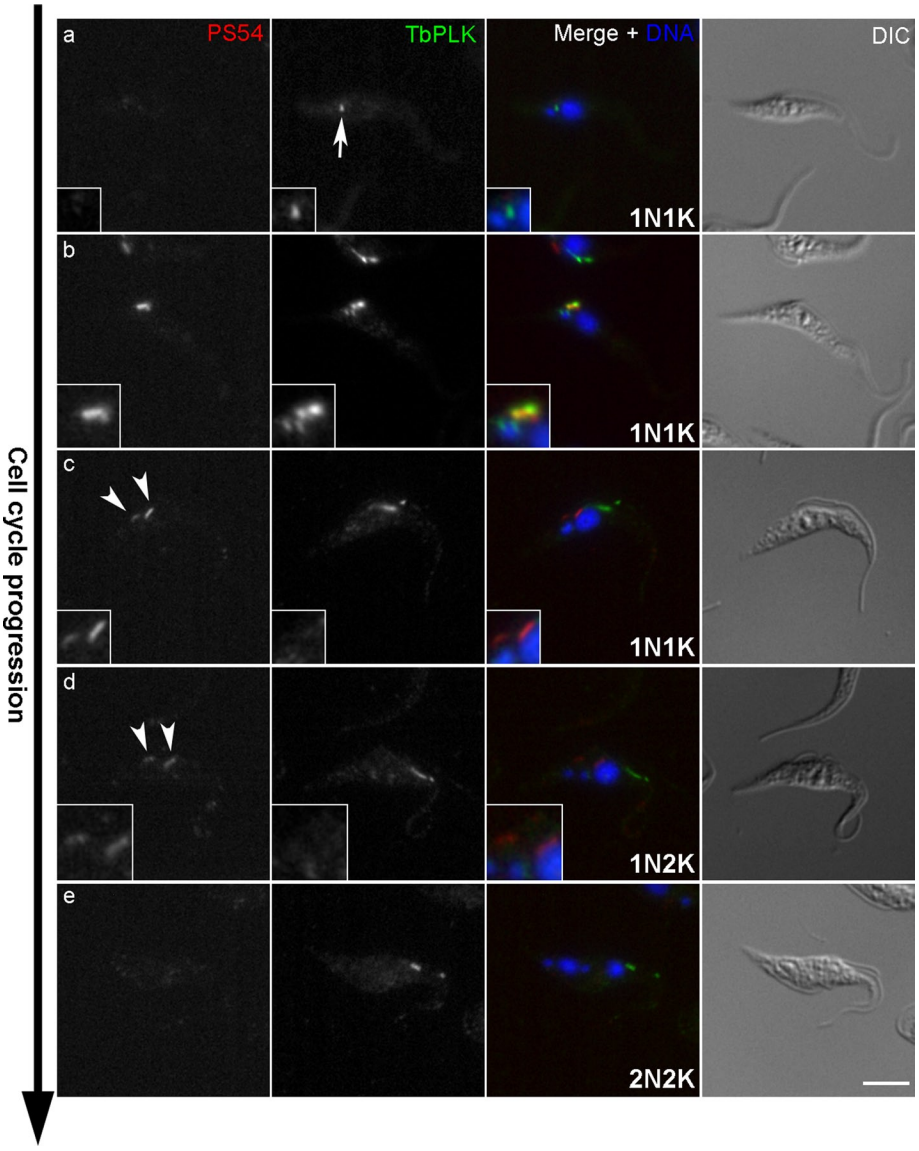

FIGURE 5: PS54 labeling occurs when TbPLK is present on the bilobe. Methanol-fixed cells were stained with PS54 (PS54; red), anti-TbPLK (TbPLK; green), and DAPI (DNA; blue) and imaged by fluorescence and DIC microscopy. The inserts show a twofold magnification of the bilobe region of each cell. TbPLK is first seen as a single punctate structure that marks the appearance of the new microtubule quartet (a, arrow). Cells with this labeling are not PS54 positive. Once PS54 labeling is apparent (b), TbPLK colocalizes with this labeling. Once the new PS54 structure appears (c, arrowheads), the TbPLK signal has migrated toward the anterior of the cell. Once kinetoplast duplication occurs (d), TbPLK has moved further away and the PS54 signal begins to decrease. PS54 labeling is not seen in 2N2K cells (e). Scale bar: 5 μm.

TbCentrin2 allele. A copy of the TbCentrin2 gene was synthesized wherein all the codons were recoded to facilitate the introduction of the mutations (Figure S6). The recoded TbCentrin2 was also tagged with a hemagglutinin (HA) tag so that it could be distinguished from the doxycycline-inducible copy of the gene. The recoded gene was used to replace the remaining TbCentrin2 allele in the presence of doxycycline, such that the cells had a supply of normal protein. Doxycycline was then removed from the medium to shut off expression of the normal protein, leaving the recoded allele as the only source of TbCentrin2 in the cell. The viability of the system was tested by introducing nonmutated, recoded TbCentrin2 into cells and removing doxycycline (Figure 6A). These cells grew in a manner identical to that of the cells supplemented with doxycycline, showing that the recoded allele was capable of supporting growth at the endogenous locus.

Once the complemented conditional knockout approach was validated, we replaced the second allele of TbCentrin2 with a recoded copy containing S54 mutations. The residue was mutated to either alanine to block phosphorylation or to aspartate to mimic constitutive modification of the site. Doxycycline was removed from the complemented conditional knockout cells and their ability to grow with only the mutated TbCentrin2 was evaluated (Figure 6A). The S54A mutation caused a slow growth defect of ~30% after 6 d, while the S54D mutant ceased to divide after 5 d.

Western blotting of cell lysates from the S54A and S54D complemented conditional knockouts taken up to 8 d after removal of doxycycline showed rapid down-regulation of the wild-type Ty1-TbCentrin2, which could not be detected within 24 h of washout (Figure 6B). Immunofluorescence with an anti-Ty1 antibody showed small quantities of wild-type protein present on the basal bodies and flagellum until day 3 (unpublished data). The HA-tagged, recoded allele that contains the mutations was up-regulated in cells lacking doxycycline, slightly in the S54A cells and substantially in the S54D cells. Additional HA-reactive bands appeared in the washout cells at slightly higher molecular weights, which may reflect additional phosphorylation or other posttranslational modifications.

The DNA state of the cells expressing the S54A and S54D mutants was assessed to determine whether there were any cell cycle defects that could explain the growth phenotypes (Figure 6C). Both cell lines showed a normal DNA distribution when grown in the presence of doxycycline, with ~80% of cells in the 1N1K state, and ~20% split between the 1N2K and 2N2K states. When expression of the wild-type protein was turned off by removal of doxycycline, both mutants showed significant defects. In cells expressing only the S54A mutant for 6 d, the number of 1N1K cells dropped from 78 to 60% and the number of 2N2K cells doubled. Cells with aberrant DNA content, such as 2N1K and anucleate 0N1K cells, began to appear. Multinucleate cells were also seen, suggesting that cells were having difficulty undergoing cytokinesis. Cells expressing only the S54D mutant for 3.5 d had a more severe phenotype. The number of 1N1K cells dropped from 78 to 53%, the number of 1N2K cells decreased, and the number of 2N2K cells doubled. Aberrant DNA states were more common, including 2N1K cells, which comprised ~15% of the total population. Anucleate and multinucleate cells were also evident.

The localization of the S54 mutants was established to determine whether changes in TbCentrin2 positioning could explain the growth defects. It is possible that phosphorylation of S54 is necessary for proper recruitment of TbCentrin2. Alternatively, the S54A

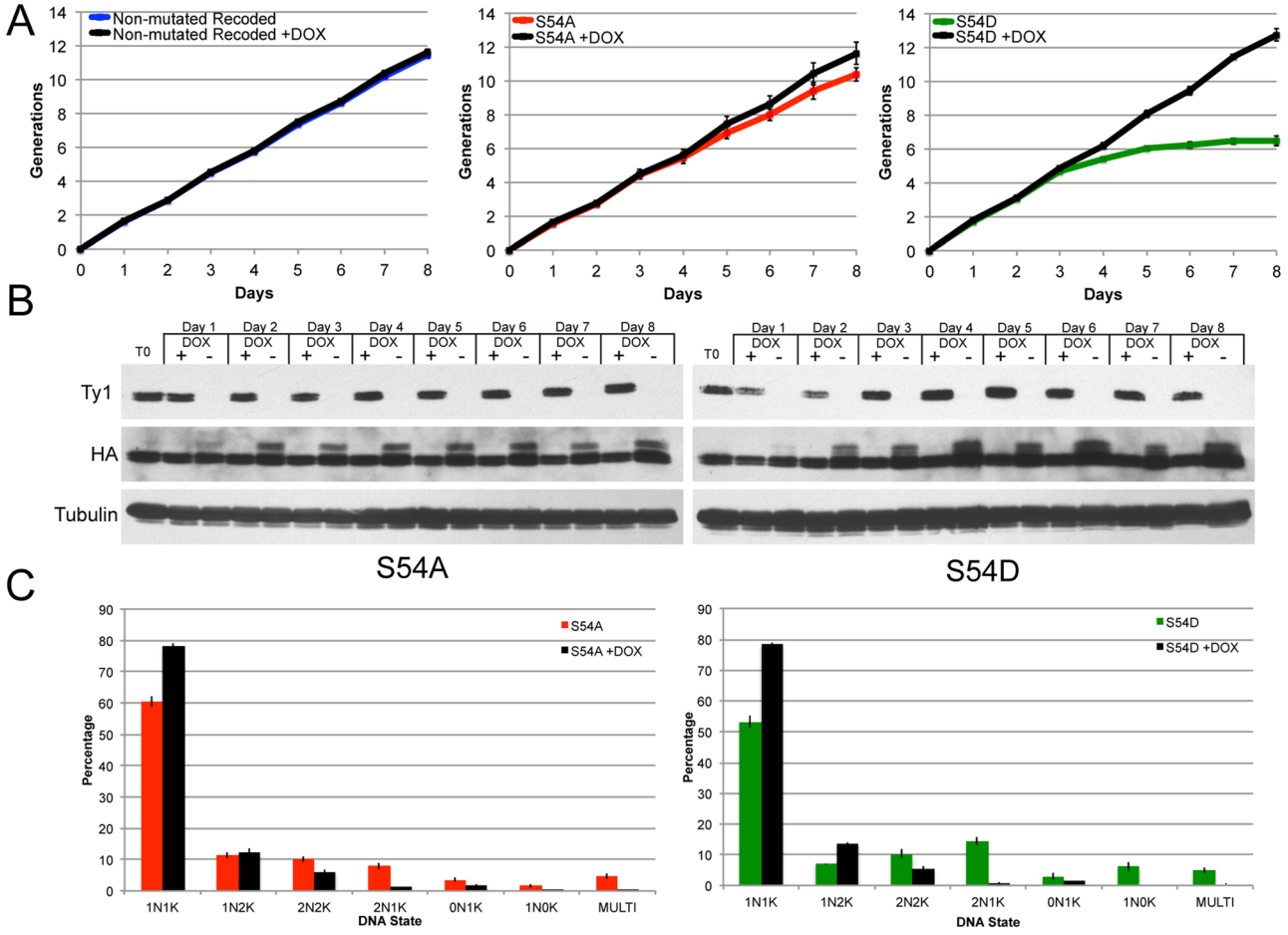

FIGURE 6: Mutation of Ser-54 in TbCentrin2 causes defects in cell division. (A) Complemented conditional knockout cells complemented with nonmutated recoded TbCentrin2 (Non-mutated Recoded; blue), S54 mutated to alanine (S54A; red), or S54 mutated to aspartate (S54D; green). The cell lines were grown in the presence (black line) or absence (colored line) of doxycycline, and the growth of the cultures was monitored by cell counting. (B) Complemented conditional knockout cell lines carrying the TbCentrin2 S54A and S54D mutations were grown over the course of 8 d with and without doxycycline. Cells from each culture were harvested daily and subjected to Western blot analysis. T0 represents the culture at the start of each experiment. The top blots show the levels of the wild-type Ty1-TbCentrin2, the middle blots show the levels of the recoded HA-TbCentrin2, and the bottom blots show the levels of tubulin. (C) Complemented conditional knockout cell lines that carry the TbCentrin2 S54A and S54D mutations were grown with or without doxycycline for 6 d in the case of S54A (red) and 2.5 d in the case of S54D (green). The cells were fixed and stained with DAPI to establish their DNA state, which was analyzed by DIC and fluorescence microscopy.

or S54D mutants might disrupt the protein so that it can no longer fold and localize properly. The HA-tagged wild-type and S54 mutants at the endogenous loci showed basal body and flagellum labeling, but due to low expression levels, it was difficult to identify the bilobe pool of the protein (unpublished data). To ensure that the TbCentrin2 mutants were still capable of targeting correctly, we transiently overexpressed the proteins as green fluorescent protein (GFP) fusions and generated extracted cytoskeletons. Wild-type TbCentrin2 and the two S54 mutants localized to the basal body, bilobe, and flagellum, emphasizing that the mutation had no effect on localization (Figure 7, A–C).

Mutations of TbCentrin2 S54 cause defects in bilobe and FAZ duplication

The status of the bilobe was evaluated in S54A and S54D complemented conditional knockout cells. Considering that S54 phosphorylation, as marked by PS54, occurs on the bilobe, it seemed possible that the growth defects observed in the S54 mutants were due to problems with replicating this structure. The complemented conditional knockout cells were grown with or without doxycycline for 3.5 d for S54D and 6 d for S54A, then fixed and stained for the bilobe and basal body component TbCentrin4 (Figure 8). In control cells expressing normal TbCentrin2, bilobe duplication occurred in 1N1K cells and was followed by separation of the duplicated structures during the 1N2K and 2N2K states (Figure 8, A, a–d, and B). Bilobe duplication does not occur properly in cells expressing the S54 mutants. The number of 1N1K cells with two bilobes decreased from 9 to 3% in the S54D mutant, although many cells still displayed elongated bilobes that appeared similar to duplication intermediates (Figure 8B). The number of cells with two bilobes also declined slightly in the S54A mutant. The 1N2K cells with single bilobes, which never appeared in the control sample, became evident (Figure 8, A, e, and B), along with cells in which the bilobe morphology was perturbed, which we referred to as malformed (Figure 8B). In 2N2K cells, 11% of S54A and S54D cells had single bilobes, although TbCentrin4 labeling near both kinetoplasts occurred frequently,

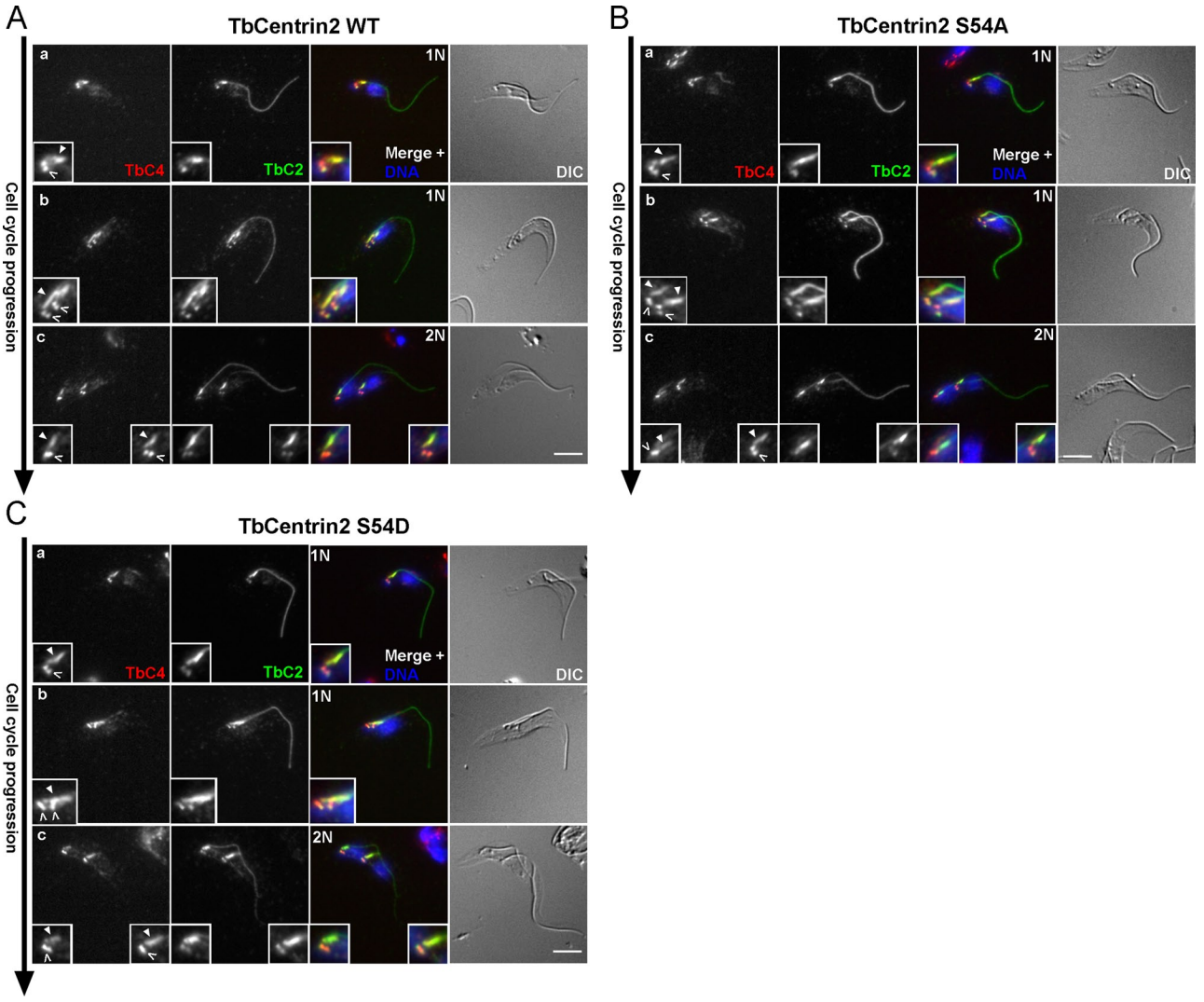

FIGURE 7: The TbCentrin2 S54 mutants have the same localization as the wild-type protein. Cells were transfected with GFP-tagged wild-type, S54A, or S54D TbCentrin2 (TbC2; green), followed by the preparation of isolated cytoskeletons, which were stained with anti-TbCentrin4 (TbC4; red) and DAPI (DNA; blue). The cytoskeletons were imaged by fluorescence and DIC microscopy. The inserts represent a twofold magnification of the bilobe region, with the basal body marked with an open arrowhead and the bilobe marked with a solid arrowhead. Nonmutated TbCentrin2 localized to the basal body, bilobe, and flagellum. The S54A and S54D mutants localized to the same structures. Scale bars: 5 μm.

suggesting that basal body duplication had proceeded normally (Figure 8, A, f, open arrowhead, and B). The 2N2K cells with malformed bilobes also comprised 26% of the S54A and 52% of the S54D populations (Figure 8, A, g, arrow and B). The 2N1K cells had severe defects in bilobe duplication, with 70% of the S54A and 80% of the S54D populations having a single bilobe (Figure 8, A, h, and B). We occasionally observed 1N1K cells that appeared to lack any organized bilobe staining (Figure 8, A, i, and B). The severity of the phenotypes tended to be higher in the S54D cells, which is consistent with the strength of the growth defect.

We next tested the effect of the S54 mutations on the assembly of a new FAZ. Complemented conditional knockout cells were grown under the same conditions as in the bilobe experiment and then labeled for the FAZ component, FAZ1. In cells expressing wild-type TbCentrin2, new FAZ formation is evident in 18% of 1N1K cells (Figure 9, A, a–b, arrowheads, and B). The new FAZ continues to elongate in the 1N2K and 2N2K states (Figure 9, A, c–d, arrowheads, and B). In cells expressing only the S54 mutants, new FAZ assembly was impeded. The 1N1K cells with detached new flagella were visible, indicating new FAZ formation was impeded, although the number of cells with new FAZ was not decreased in the S54 mutants (Figure 9A, e, arrowhead). The 1N2K cells that had only one FAZ comprised 16% of the S54A and 20% of the S54D populations. We also observed 1N2K cells that contained punctate new FAZ, which we termed short new FAZ (snFAZ), and had detached new flagella (Figure 9, A, f, arrowhead, and B). In the 2N2K state, 21% of S54A and 56% of S54D cells contained snFAZ shorter than 5 μm, which was the shortest length for a new FAZ observed in cells expressing nonmutated TbCentrin2 (Figure 9, A, g, arrowhead, and B). Some 2N2K cells totally lacked new FAZ (Figure 9B). In the aberrant 2N1K cells, 69% of S54A and 59% of S54D cells had a single FAZ, while the remaining cells had an snFAZ (Figure 9, A, h, and B). Most cells with FAZ defects also had detached new flagella (Figure 9A, e–g, arrows). We also observed 1N1K cells in which the only FAZ was abnormally short, which we termed short old FAZ (soFAZ; Figure 9, A, i, and B). These cells frequently had fully or partially detached flagella.

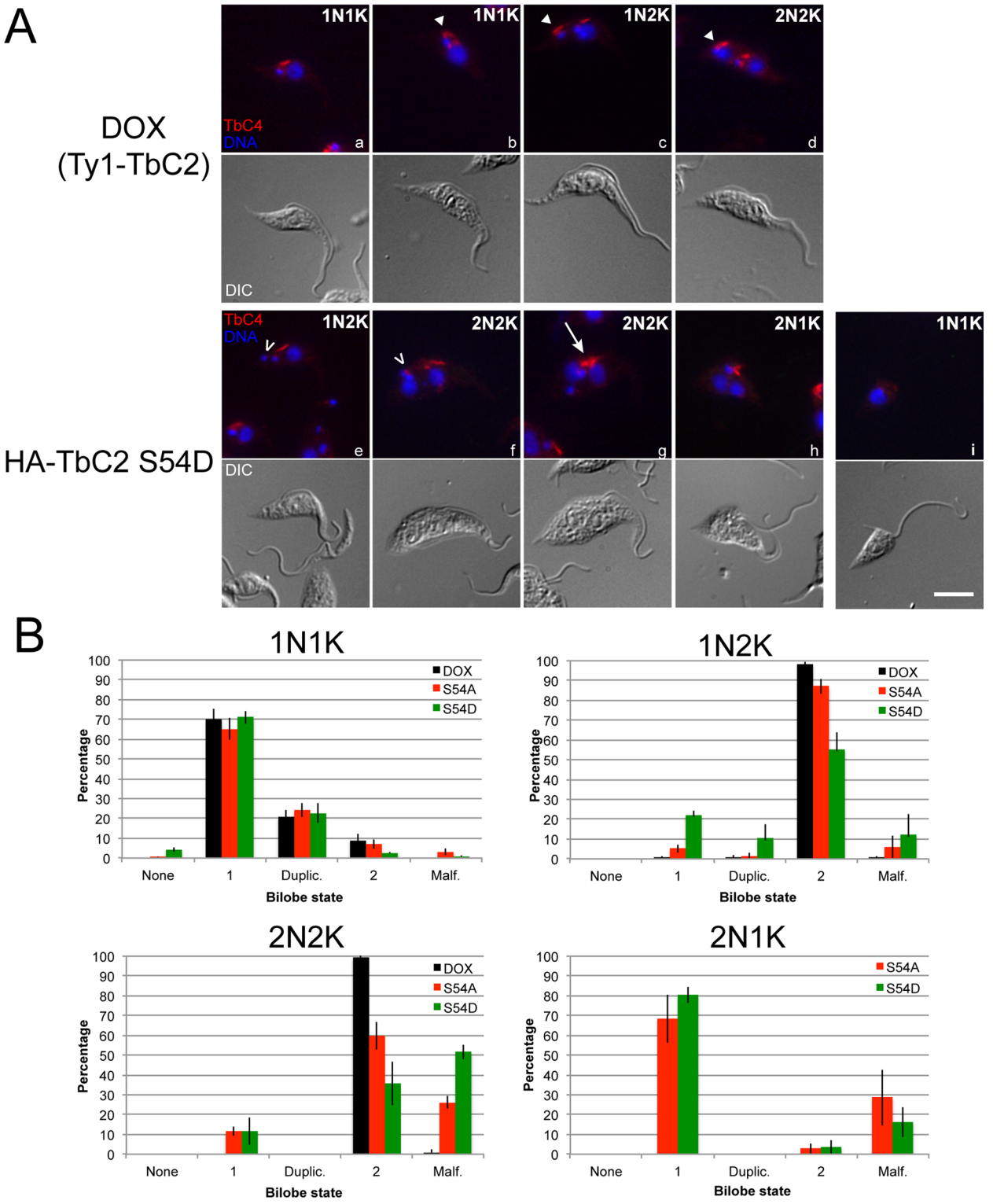

FIGURE 8: Mutation of TbCentrin2 S54 causes defects in bilobe duplication. (A) Complemented conditional knockout cells carrying the S54A or S54D mutation were grown in the presence or absence of doxycycline for 6 d (S54A) or 3.5 d (S54D). The cells were then fixed and labeled with anti-TbCentrin4 (TbC4; red), and DAPI (DNA; blue). Cells from the S54D data set are shown. Cells incubated with doxycycline (DOX) express nonmutated Ty1-TbCentrin2, while the cells without doxycycline express only the mutant HA-tagged TbCentrin2 (HA-TbCentrin2 S54D). In control conditions, bilobe duplication began in 1N1K cells (b, arrowhead), followed by the separation of the duplicated structures in 1N2K and 2N2K cells (c and d, arrowheads). In cells expressing only mutant TbCentrin2, 1N2K and 2N2K cells lacking new bilobes appeared (e and f, open arrowheads). Cells with malformed bilobes also appeared (g, arrow). (B) Quantification of the bilobe phenotype seen in (A). The results for the S54A cells are in red, the results for the S54D cells in green, and the results for the control cells are in black (DOX). Each graph shows the results for cells at a specific DNA state. 2N1K cells are only present in the cultures lacking doxycycline. Scale bar: 5 μm.

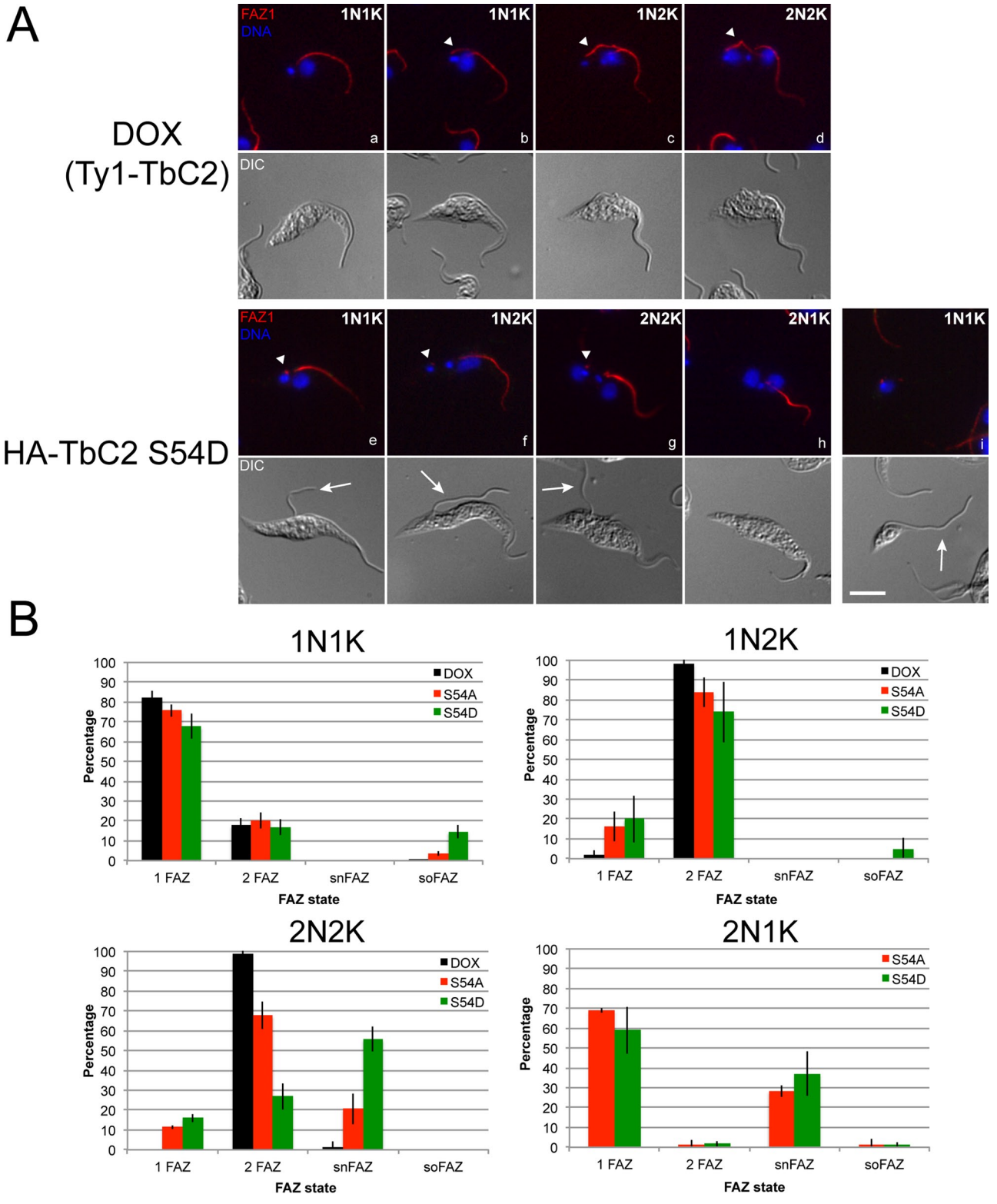

FIGURE 9: Mutation of TbCentrin2 S54 causes defects in FAZ duplication. (A) Complemented conditional knockout cells carrying the S54A or S54D mutation were grown in the presence or absence of doxycycline for 6 d (S54A) or 3.5 d (S54D). The cells were then fixed and labeled with anti-FAZ1 (FAZ; red) and DAPI (DNA; blue). Cells incubated with doxycycline (DOX) express nonmutated Ty1-TbCentrin2, while the cells without doxycycline express only the mutant HA-tagged TbCentrin2 (HA-TbCentrin2 S54D). In the control sample, FAZ duplication occurred in 1N1K cells (b, arrowhead), followed by extension of the new structure in 1N2K and 2N2K states (c and d; arrowhead). In cells expressing the TbCentrin2 S54 mutants, new FAZ synthesis was perturbed. Cells had punctate snFAZ (e–g, arrowheads) or lacked new FAZ entirely (h). (B) Quantification of the FAZ phenotype seen in (A). The results for the S54A cells are in red, the results for the S54D cells in green, and the results for the control cells are in black (DOX). Each graph shows the results for cells at a specific DNA state. 2N1K cells are only present in the cultures lacking doxycycline. Scale bar: 5 μm.

While studying the bilobe and FAZ states in the S54 complemented conditional knockouts, we noted by differential interference contrast microscopy (DIC) that 2N2K and 2N1K cells occasionally appeared to lack two flagella. This differs markedly from the result of TbPLK depletion, in which all 2N2K and 2N1K cells contain two flagella (Ikeda and de Graffenried, 2012). The two possibilities are either that new flagellar assembly may be compromised or aberrant cytokinesis may lead to the production of cells that contain a flagellum but lack the correct complement of DNA. If the S54 mutants cause defects in flagellar assembly, then cells at all cell cycle stages should lack new flagella. However, if the lack of new flagella is confined to later stages of the cell cycle, this defect is likely due to aberrant cytokinesis that leads to a loss of a flagellum.

For testing these two possibilities, complemented conditional knockout cells were grown as in the bilobe and FAZ experiments and stained with an antibody against the paraflagellar rod component PFR2 (Kohl *et al.*, 1999). The number of flagella in cells expressing nonmutated and mutant TbCentrin2 were then counted in all cell cycle states. In cells expressing nonmutated TbCentrin2, the new flagellum appeared in 17% of 1N1K cells and continued to elongate throughout the rest of the cell cycle (Figure 10, A, b–d, arrowheads, and B). Cells expressing the TbCentrin2 mutants did not appear to have flagellar defects early in the cell cycle. In 1N1K cells, the S54 mutants had a slightly elevated number of cells with two flagella, 20% in the S54A and 25% in the S54D mutant, which argues that there is no defect in assembly of new flagella (Figure 10, A, e, arrowhead, and B). In the 1N2K state, cells lacking a new flagellum comprised 4% of the population in the S54A mutant and 16% in the S54D mutant (Figure 10, A, f, and B). In 2N2K cells, the defect was more severe, with 7% of the S54A and 20% of the S54D mutants lacking new flagella (Figure 10, A, g, and B). In 2N1K cells, the absence of new flagella was very evident, with 66% of the S54A and 46% of the S54D cells containing only one flagellum (Figure 10, A, h, and B). In cells that lacked new flagella, the old flagella were almost always attached.

DISCUSSION

The original localization of TbCentrin2 was described using the 20H5 monoclonal antibody, which was raised against *Chlamydomonas* centrin (Sanders and Salisbury, 1994).The 20H5 monoclonal antibody detects centrins in many organisms and appears to recognize the amino acid sequence ElxxAFxLFD, a motif present in many EF hands, explaining its generality (Klotz *et al.*, 1997). Previous work in trypanosomes has shown that 20H5 detects both TbCentrin1 and TbCentrin2 (He *et al.*, 2005). Endogenous tagging experiments showed that TbCentrin1 localized exclusively to the basal body, while TbCentrin2 localized to the bilobe and the basal body. This made it likely that the bilobe signal produced by 20H5 was attributable to TbCentrin2.

We have produced a new monoclonal antibody that is specific for TbCentrin2 due to its recognition of a segment of the N-terminus, which is one of the few regions in which centrins show variability. When this antibody is used for immunofluorescence with methanol fixation, it predominantly labels the basal body and flagellum, with modest bilobe labeling. Extraction with detergent prior to fixation enhances the bilobe pool, perhaps by exposing more antigenic sites. The amount of TbCentrin2 on the bilobe seems exquisitely sensitive to its expression level in cells; overexpression of GFP-TbCentrin2 leads to a readily detectable bilobe pool. It is possible that tagging both alleles with Ty1, as was done previously, elevates the expression level of the protein sufficiently to increase its presence on the bilobe (He *et al.*, 2005). It is also possible that phosphorylation of the N-terminus of TbCentrin2 blocks 2B2H1 binding, although preliminary experiments with phosphatase treatments did not show any additional labeling upon treatment. Based on our data, it is likely that, when expressed at endogenous levels, TbCentrin2 resides mostly on the basal body and flagellum, with a portion present on the bilobe.

TbCentrin2 is phosphorylated on multiple residues in *T. brucei*. Mass spectrometry analysis identified 12 different phosphosites in TbCentrin2 purified from cells. A previous study on the whole-cell phosphoproteome of bloodstream-form trypanosomes identified only one of these sites, S10, which appears to be abundant (Nett *et al.*, 2009b). Many of the sites were only identified after TiO_2 enrichment of the purified TbCentrin2 phosphopeptides, suggesting they were not heavily occupied in an asynchronous culture. This may be due to the fact that they are only present at certain points in the cell cycle. The N-terminal extension of TbCentrin2 is heavily phosphorylated, and these sites appear to be occupied simultaneously, because peptides with more than one phosphorylated residue were identified. Deletion of the N-terminal extension did not have any effect on the localization of TbCentrin2 or cell viability (unpublished data), which is consistent with similar experiments conducted on the yeast homologue Cdc31p (Li *et al.*, 2006).

Among the phosphosites mapped on TbCentrin2, two have been identified previously in other organisms. Human Centrin2 is phosphorylated on the S54 equivalent (S47) in vitro by the kinase Mps1 (Yang *et al.*, 2010). Overexpression of S54 mutants had a modest effect on centriole overproduction in S phase–arrested cells, but viability was not tested. T142, which is phosphorylated by TbPLK in vitro, is modified in the yeast centrin homologue Cdc31p (T110) and in human Centrin2 by Mps1 (Araki *et al.*, 2010; Yang *et al.*, 2010). While we were not able to identify T142 phosphorylation in vivo, it is possible that it is present at levels below our detection. It is not surprising that Mps1 and PLK homologues would phosphorylate similar sites, as they both recognize acidic sequences and may associate in some organisms (Mok *et al.*, 2010; Dou *et al.*, 2011). No Mps1 homologue has been identified in the trypanosome genome.

A phosphospecific antiserum raised against TbCentrin2 S54 labels the bilobe as the structure is undergoing duplication. This labeling pattern coincides with the appearance of TbPLK on the bilobe and rapidly decreases once the kinase has migrated onto the tip of the new FAZ. This is consistent with the bilobe pool of TbCentrin2 serving as a substrate for TbPLK and indicates this event serves as a clear marker for the onset of bilobe duplication. The appearance of the PS54 signal occurs prior to the assembly of a new bilobe and FAZ filament. Soon after the bilobe becomes PS54-positive, a new PS54-labeled structure appears just to the posterior of the old bilobe and a new FAZ can be seen. This could mean that a phosphorylation event on the old bilobe is necessary to assemble a new bilobe, perhaps by liberating or recruiting a TbCentrin2-binding protein. Recent work has shown that the TbCentrin2 levels on the bilobe do not change during the cell cycle, making it unlikely that TbPLK phosphorylation changes the localization of TbCentrin2 (Wang *et al.*, 2012). The TbCentrin2 S54A and S54D mutants both have the same localization as the wild-type protein.

The disappearance of the PS54 epitope after bilobe duplication suggests that one or more phosphatases are responsible for removing TbPLK phosphorylation from TbCentrin2 at a specific point in the cell cycle. The identity of this phosphatase is currently unknown, but considering the consequences of mimicking constitutive phosphorylation of S54, its action is a vital event in cell division in *T. brucei*. Very little is known about the phosphatases present in trypanosomes beyond the role of TbPTP1 in the differentiation of the parasite (Szöör *et al.*, 2006; Szöör, 2010). It should also be noted

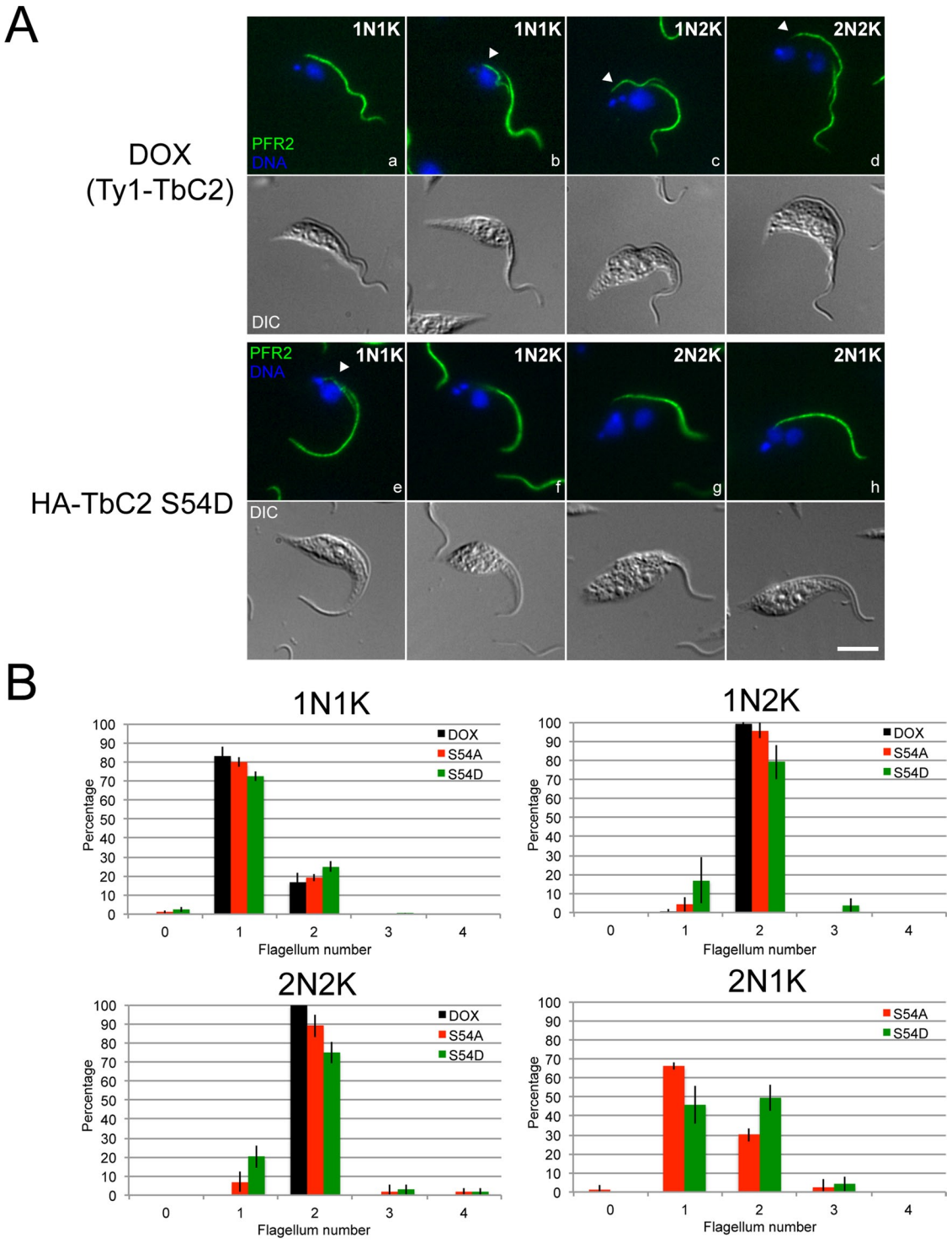

FIGURE 10: Mutation of TbCentrin2 S54 does not affect the assembly of new flagella. (A) Complemented conditional knockout cells carrying the S54A or S54D mutation were grown in the presence or absence of doxycycline for 6 d (S54A) or 3.5 d (S54D). The cells were then fixed and labeled with anti-PFR2 (PFR2; green) and DAPI (DNA; blue). Cells from the S54D data set are shown. Cells incubated with doxycycline (DOX) express nonmutated Ty1-TbCentrin2, while the cells without doxycycline express only the mutant HA-tagged TbCentrin2 (HA-TbCentrin2 S54D). In the control sample, new flagellum assembly initiated in 1N1K cells, followed by extension of the new structure in the 1N2K and 2N2K states (b–d, arrowheads). In cells expressing the TbCentrin2 mutants, new flagellum initiation occurred in 1N1K cells (e, arrowhead), but cells that had progressed further in the cell cycle occasionally lacked new flagella (f–h). (B) Quantification of the flagellum phenotype seen in (A). The results for the S54A cells are in red, results for the S54D cells are in green, and results for the control cells are in black (DOX). Each graph shows the results for cells at a specific DNA state. 2N1K cells are present only in the cultures lacking doxycycline. Scale bar: 5 μm.

that PLK homologues in other organisms are targeted by the action of upstream kinases, which generate phosphosites that bind the polo-box domain of PLK (Elia *et al.*, 2003; Barr *et al.*, 2004). Considering the migration of TbPLK throughout the cell cycle, it is likely that several kinases and phosphatases are tasked with generating and removing phosphosites to target TbPLK to specific cellular locations at specific moments during division.

Mutation of S54 to alanine or aspartate causes defects in the assembly of the bilobe and FAZ. The organelles impacted by the S54 mutation are consistent with the location of the PS54 signal, which argues that the phenotypes are due to interfering with phosphorylation of this site. The alanine mutation causes a slow-growth phenotype, which may mean that the phosphorylation event is not essential. Mutating S54 to aspartate causes cell division to cease, which suggests that once the site has been occupied it must be removed for bilobe and FAZ assembly to continue. In the S54 mutants, 20% of 2N2K cells have only one flagellum, while almost half of the 2N1K cells have the same phenotype. The absence of a new flagellum can occur by two mechanisms: basal body maturation can be compromised, blocking the assembly of a new flagellum, or aberrant cytokinesis can produce cells that contain flagella but lack the appropriate DNA. If flagellum assembly is perturbed, a decrease in 1N1K cells with two flagella would be expected, but this is not the case in the S54 mutants. The loss of flagella appears to occur later in the cell cycle, which would be consistent with a defect in cytokinesis. This defect could be due to premature cytokinesis, wherein furrow ingression occurs prior to the correct arrangement of the kinetoplasts, or by misplacement of the furrow. New FAZ assembly may play an important role in directing the placement of the cleavage furrow, which could explain why the S54 mutants are producing cells with cytokinetic defects (Robinson *et al.*, 1995; Kohl *et al.*, 2003; Vaughan, 2010). While cells expressing the TbCentrin2 S54 mutants appear to produce a new flagellum as detected by the paraflagellar rod component PFR2, it should be noted that PFR2 is not a component of the axoneme and does not extend along the full length of the flagellum. This raises the possibility that the new flagella are not fully functional or are shorter than in cells expressing nonmutated TbCentrin2.

The precise mechanism for how S54 phosphorylation affects bilobe and FAZ assembly is under investigation. The S54 site is present within the first EF hand and is positioned within the coordination sphere of the calcium ion. Phosphorylation of this site could cause a decrease in calcium binding due to the negative charge and bulk of the phosphate moiety. Phosphorylation of Centrin2 by CK2 in vertebrate photoreceptor cells causes a fivefold decrease in calcium binding (Trojan *et al.*, 2008). However, previous work with human Centrin2 has shown that the first two EF hands have millimolar affinity and would not be populated at normal cellular concentrations of free calcium (10^{-7}–10^{-5} M; Yang *et al.*, 2006).

In calmodulin, calcium binding leads to a conformational change that exposes a binding surface and allows it to bind to other proteins. In TbCentrin2, it is possible that the first two EF hands do not bind calcium, but may instead serve as protein-binding modules. These EF hands are found in the closed state in the crystal structure of human Centrin2, making it possible that phosphorylation at S54 drives a conformational change that exposes a novel binding surface (Thompson *et al.*, 2006). If this is the case, then phosphorylation of this site by TbPLK may serve to recruit a binding partner at a specific point in the cell cycle. Recruitment of this binding partner may facilitate bilobe duplication, but it may not be absolutely essential for this process, or it could be recruited by another pathway that does not require the kinase. If the binding partner is recruited, it must be released or relocated to allow bilobe duplication to proceed. By mimicking constitutive phosphorylation of this site, we can block new bilobe assembly, which leads to FAZ defects and detached flagella, and blocks cytokinesis from proceeding properly.

MATERIALS AND METHODS

Cell culture

All experiments were performed using the procyclic *T. brucei* cells. The 427 strain was used to produce the TAP-TbCentrin2 cell line, along with all immunofluorescence conducted on wild-type cells. The 427 cells were grown in SDM-79 supplemented with 7.5 μg/ml hemin and 20% fetal calf serum (FCS). The complemented conditional knockout strains were generated in the 29.13 cell line (Wirtz *et al.*, 1999). The 29.13 cells were grown in SDM-79 supplemented with 7.5 μg/ml hemin, 20% Tet-System approved FCS (Clontech, Mountain View, CA), 15 μg/ml neomycin, and 50 μg/ml hygromycin. All cells were cultured at 27°C, and their growth was monitored using a particle counter (Z2 Coulter Counter; Beckmann Coulter, Brea, CA).

Antibodies

Antibodies were obtained from the following sources: anti-FAZ1 (L3B2) and anti-PFR2 (L8C4) from Keith Gull (Oxford University, UK), anti–*Leishmania donovani* Centrin4 from Hira L. Nakhasi (U.S. Food and Drug Administration), anti-Ty1 (BB2) from Cynthia He (National University of Singapore, Singapore), anti-GFP from Egon Ogris (Max F. Perutz Laboratories, Vienna, Austria). The mouse monoclonal anti-HA (clone 16B12; Covance, Princeton, NJ), anti–α-tubulin (clone B-5-1-2; Sigma-Aldrich, St. Louis, MO), and anti-His_6 (GE Healthcare, Waukesha, WI) were purchased from the respective companies. The monoclonal antibodies against TbCentrin2 and TbCentrin4 and the rabbit polyclonal against TbPLK have been described previously (de Graffenried *et al.*, 2008; Ikeda and de Graffenried, 2012). The rat monoclonal against TbPLK was generated against a C-terminal fragment corresponding to the polo-box domain (aa 468–768) expressed in *E. coli* as a His_6-fusion. The specificity of this antibody is shown in Figure S7. The phosphospecific rabbit antiserum PS54 was generated against the peptide FDTDG(S)GTIDVKELC fused to KLH. The resultant serum was purified against the phosphorylated peptide and then absorbed against the unphosphorylated version prior to use.

Immunofluorescence

Cells were harvested, washed once in phosphate-buffered saline (PBS), and then adhered to coverslips. For direct methanol fixation, the cells were then immersed in –20°C methanol for 20 min, air-dried, and then rehydrated in PBS. For extracted cytoskeletons, the cells on coverslips were incubated in extraction buffer (0.1 PIPES, pH 6.9, 2 mM EGTA, 1 mM $MgSO_4$, 0.1 M EDTA, 1% NP40) for 5 min at room temperature and washed in PBS three times; this was followed by fixation in –20°C methanol for 20 min and rehydration in PBS. The cells were blocked overnight at 4°C in blocking buffer (PBS containing 3% bovine serum albumin). Primary antibodies were diluted in blocking buffer and incubated for 1 h at RT, and then washed four times in PBS and placed in blocking buffer for 20 min. Alexa 488– or 568–conjugated secondary antibodies were diluted in blocking buffer and incubated for 1 h at RT. Cells were washed and mounted in Fluoromount G with 4′,6-diamidino-2-phenylindole (DAPI; Southern Biotechnology, Birmingham, AL). Coverslips were imaged using a custom-built epifluorescence microscope (Observer Z1; Zeiss, Jena, Germany) equipped with a pco. 1600 camera (pco., Romulus, MI) and a Plan-Apochromat 100×/1.46 oil-immersion lens (Zeiss). Visiview (Visitron Systems) was used to control the microscope

for acquisition. All images were quantified in ImageJ and assembled for publication using Photoshop CS5 and Illustrator CS5 (Adobe, San Jose, CA).

Western blotting

Cells were harvested, washed once in PBS, and then lysed in SDS–PAGE loading buffer. Samples containing 3×10^6 cell equivalents of lysate per lane were fractionated using SDS–PAGE, transferred to nitrocellulose, and probed with primary antibodies. Detection was performed using secondary antibodies conjugated to horseradish peroxidase (Jackson ImmunoResearch, West Grove, PA) and film. In certain cases, the nitrocellulose membranes were stripped using Restore (Pierce Biotechnology, Rockford, IL) and reprobed with a different primary antibody.

Construction of TAP-TbCentrin2 cell line

Cells (1×10^8) were transfected with a construct containing the puromycin resistance gene flanked by 500 bp of the 5′ and 3′ untranslated regions (UTRs) of TbCentrin2. Resistant clones were isolated, and integration of the puromycin resistance gene at the TbCentrin2 loci was confirmed by PCR. A suitable clone was selected and transfected with a TbCentrin2-targeted tagging construct that introduced a TAP-tag at the N-terminus of the gene and a gene conferring blasticidin resistance. Double integrants were cloned and screened by PCR. The absence of untagged TbCentrin2 was confirmed by blotting the resultant clones with anti-TbCentrin2 antibody.

TAP-tag purification

Cells (5×10^9) were harvested, washed once in PBS, and then lysed in 5 ml of a modified RIPA buffer (50 mM Tris, pH 7.4, 150 mM NaCl, 2 mM EDTA, 1% NP40, 0.1% SDS, 1 tablet per 25 ml Complete protease inhibitor, 1 tablet PhosSTOP phosphatase inhibitors [Roche, Basel, Switzerland]) containing 3 M urea. The lysate was vortexed frequently and kept at 4°C for 30 min, and then clarified by centrifugation at 16,000 × *g* for 30 min at 4°C. The clarified lysate was diluted to 50 ml in modified RIPA buffer lacking urea, and incubated with 100 µl bed volume of immunoglobulin G beads for 3.5 h at 4°C. The beads were washed in modified RIPA buffer and then resuspended in TEV cleavage buffer (25 mM Tris, pH 8.0, 150 mM NaCl, 0.1% NP40, 0.5 mM EDTA, 1 mM DTT). TEV protease was added, and the beads were incubated overnight at 4°C. The bed eluate was collected, along with two washes, and $CaCl_2$ was added to bring the concentration to 2 mM. The eluate was then diluted in calmodulin-binding buffer (25 mM Tris, pH 8.0, 150 mM NaCl, 1 mM magnesium acetate, 1 mM imidazole, 2 mM $CaCl_2$, 10 mM β-mercaptoethanol) and incubated with 60 µl bed volume of calmodulin beads for 1.5 h. The beads were washed in calmodulin-binding buffer with 0.1% NP40, followed by 0.02% NP40. Samples for TiO_2 enrichment were trypsinized directly from the beads, while those that were processed from gel slices were eluted with calmodulin elution buffer (25 mM Tris, pH 8.0, 150 mM NaCl, 0.2% NP40, 1 mM magnesium acetate, 1 mM imidazole, 20 mM EGTA, 10 mM β-mercaptoethanol). The eluate was concentrated and then boiled in SDS–PAGE loading buffer. The sample was then fractionated on a NU-PAGE 4–12% gel and stained using SimplyBlue Coomassie stain (Invitrogen, Carlsbad, CA). The only band present had the correct MW for TbCentrin2 fused to the calmodulin-binding peptide. This band was excised and submitted for LC-MS/MS analysis.

Kinase assays

The kinase assay protocol was adapted from a previously published protocol (Hammarton *et al.*, 2007). Purified TbPLK or its kinase-dead mutant were mixed with 10 µg recombinant TbCentrin2 in kinase assay buffer (50 mM MOPS, pH 7.2, 20 mM $MgCl_2$, 10 mM EGTA, and 2 mM dithiothreitol [DTT]); this was followed by the addition of 20 µM ATP and incubation for 30 min at 30 °C. Thirty percent of each reaction was fractionated using SDS–PAGE and then stained with GelCode (Thermo Scientific) to visualize proteins. The band corresponding to TbCentrin2 at 21 kDa was excised and subjected to LC-MS/MS analysis.

LC-MS/MS analysis

Coomassie-stained gel bands were excised, then washed with 50 mM NH_4HCO_3 (pH 8.5), and dried with acetonitrile. Disulfide bonds were reduced with DTT (200 µl of 10 mM DTT for 30 min at 56°C). DTT was removed, and cysteines were alkylated by incubation with 100 µl of 54 mM iodoacetamide (IAA) for 20 min at RT in the dark. Gel pieces were dried with acetonitrile, then swollen in 10 ng/µl trypsin (recombinant, proteomics grade; Roche, Indianapolis, IN) in 50 mM NH_4HCO_3, and incubated overnight at 37°C. The reaction was quenched by adding formic acid to a final concentration of ~1%, and peptides were extracted by sonication.

For phosphopeptide enrichment TbCentrin2 was digested directly from calmodulin beads used in the TAP-tag purification. The beads were washed five times with NH_4HCO_3 buffer. Disulfide bonds were reduced with DTT (5% wt/wt of the estimated amount of protein), and Cys-residues were subsequently alkylated with IAA (25% wt/wt of the estimated amount of protein) as described above. DTT (25% wt/wt of the estimated amount of protein) was added to consume excess IAA, and proteins were digested with trypsin (recombinant, proteomics grade; 5% wt/wt of the estimated amount of protein; Roche) at 37°C overnight. Digests were stopped by addition of trifluoroacetic acid (TFA) to approximately pH 2.5.

Phosphopeptide enrichment with TiO2 was performed as previously described (Mazanek *et al.*, 2007). Briefly, TopTip-TiO2 from Glygen (TT1TIO.96) were washed with 80% acetonitrile and equilibrated in a buffer containing 130 mg/ml 1-octanesulfonic acid, 100 mg/ml 2,5-dihydroxybenzoic acid, and 0.2% heptafluorobutyric acid in 40% acetic acid. The sample was dissolved in the equilibration buffer and loaded very slowly on the tips, washed, and eluted very slowly with a phosphate buffer (pH 10.5).

Peptides were separated on an UltiMate 3000 HPLC system (Dionex, Thermo Fisher Scientific). Digests were loaded on a trapping column (PepMap C18, 5 µm particle size, 300 µm i.d. × 5 mm; Thermo Fisher Scientific) equilibrated with 0.1% TFA and separated on an analytical column (PepMap C18, 3 µm, 75 µm i.d. × 150 mm; Thermo Fisher Scientific), applying a 30-min linear gradient from 2.5% up to 40% acetonitrile with 0.1% formic acid, followed by a washing step with 80% acetonitrile and 10% trifluoroethanol. The HPLC was directly coupled to an LTQ-Orbitrap Velos mass spectrometer (Thermo Fisher Scientific) equipped with a nanoelectrospray ionization source (Proxeon, Thermo Fisher Scientific). The electrospray voltage was set to 1500 V. The mass spectrometer was operated in the data-dependent mode: 1 full scan (m/z: 300–1800, resolution 60,000) with lock mass enabled was followed by maximal 20 MS/MS scans. If a neutral loss of 98, 49, or 32.6 was detected among the top three peaks, an MS3 was triggered. The lock mass was set at the signal of polydimethylcyclosiloxane at m/z 445.120025. Monoisotopic precursor selection was enabled; singly-charged signals were excluded from fragmentation. The collision energy was set at 35%, Q-value at 0.25, and the activation time at 10 ms. Fragmented ions were set onto an exclusion list for 30 s. In an additional LC-MS/MS run, CID and ETD fragmentation was triggered alternating.

Peptide identification was performed by the SEQUEST algorithm in the Proteome Discoverer 1.3.0.339 software package (Thermo Fisher Scientific). Spectra were searched against a small database containing the tagged centrin sequences plus proteases, contaminants, and a short list of unrelated proteins. Search parameters were tryptic specificity with maximum 2 missed cleavages, peptide tolerance of 2 ppm, and fragment ions tolerance of 0.8 Da. Carbamidomethylation of Cys was set as static modifications and phosphorylation of Ser/Thr/Tyr and oxidation of Met as variable modifications. Results were filtered for 1% false discovery rate, and phosphorylated peptides were checked manually. The probability of phosphosite localization was calculated using the phosphoRS2.0 software embedded in Proteome Discoverer. A phosphorylation site probability of 75% or higher was considered as confidently localized. Results were divided in confidently localized and nonlocalized (<75% probability) phosphorylation sites.

Construction of TbCentrin2 complemented conditional knockouts

The 29.13 cells were transfected with normal Ty1-TbCentrin2 in a doxycycline-inducible vector (pLEW100), and clones were selected using phleomycin (Wirtz *et al.*, 1999). Resistant clones were analyzed for the expression of Ty1-TbCentrin2, and a suitable clone was selected for further manipulation. This clone was transfected with a construct containing the blasticidin resistance gene flanked by 500 base pairs of the 5′ and 3′ UTRs of TbCentrin2. Resistant clones were isolated and integration of the blasticidin resistance gene at the TbCentrin2 loci was confirmed by PCR. A single clone was selected, which served as the parental cell line for all the complemented TbCentrin2 conditional knockouts. The parental line was transfected with recoded HA-TbCentrin2 that was targeted to the TbCentrin2 loci using the 5′ and 3′ UTRs of TbCentrin2. The transfected cells were incubated with 300 ng/ml of doxycycline and puromycin to select for the integration of the recoded HA-TbCentrin2. During the selection process, 300 ng/ml of doxycycline was added every 10 d to maintain expression of the wild-type Ty1-TbCentrin2. Isolated clones were maintained in 50 ng/ml doxycycline and screened for insertion of the recoded HA-TbCentrin2 at the correct loci by PCR. Western blotting with anti-TbCentrin2 confirmed the absence of untagged TbCentrin2. Genomic DNA from the final clones was isolated, and the sequence of the HA-TbCentrin2 was confirmed using DNA sequencing.

Induction of the complemented conditional knockouts

Complemented conditional knockout cells that were maintained with 50 ng/ml doxycycline were washed with SDM-79 media four times to remove the drug. The cells were then seeded in two flasks at 1×10^6/ml, and 50 ng/ml doxycycline was added back to one flask, while a vehicle control (70% ethanol, the solvent used to dissolve the doxycyline) was added to the other. Cells were reseeded at 1×10^6/ml every 2 d and supplemented with fresh doxycycline. Cell number was monitored using a Coulter Counter Z2.

Dephosphorylation of MeOH-fixed cells

The phosphospecificity of the PS54 antiserum was tested using an established dephosphorylation protocol (Nett *et al.*, 2009a). Cells (6×10^5 per coverslip) were washed in PBS, adhered to coverslips, fixed in –20°C MeOH for 20 min, and then air-dried and rehydrated in PBS. The coverslips were washed in NEB3 buffer (50 mM Tris, pH 7.9, 10 mM $MgCl_2$, 100 mM NaCl, 1 mM DTT) and then incubated in NEB3 buffer alone or NEB3 buffer containing 50 U of CIP. The coverslips were incubated for 16 h at 37°C and then washed with PBS and processed for immunofluorescence as described above.

Expression and purification of TbCentrin2 fragments for epitope mapping of 2B2H1

TbCentrin2 and truncations of the protein were cloned into a bacterial expression vector that generated fusion protein appending the maltose-binding protein and a His_{10} tag to their N-termini. These vectors were transformed into BL21 cells, expressed, and purified on nickel-agarose beads under denaturing conditions using 8 M urea. The concentrations of the purified proteins were measured using the BCA system (Pierce Biotechnology). An equimolar concentration of each protein was fractionated using SDS–PAGE and transferred to nitrocellulose. The membrane was probed with anti-TbCentrin2 antibody 2B2H1 and then stripped and reprobed with anti-His_6 as a loading control.

Expression and purification of recombinant proteins

TbPLK and its kinase-dead mutant were cloned into pFastBac HT as N-terminal His_6 fusions for transposition into baculovirus DNA as described by the manufacturer (Bac-to-Bac Expression system, Invitrogen). Sf9 cells were transfected with the baculovirus DNA containing the TbPLK fusions, and the resultant supernatant was used to generate high-titer virus. Hi5 cells were infected with high-titer virus and grown for 60 h to allow for TbPLK expression. The cells were lysed in Hi5 lysis buffer (20 mM HEPES, pH 7.4, 1% TritonX-100, 1% glycerol, 300 mM NaCl, 15 mM imidazole) and purified using TALON beads (Clontech) according to the manufacturer's conditions. TbCentrin2 expression and purification has been described previously (de Graffenried *et al.*, 2008).

ACKNOWLEDGMENTS

We thank all the laboratories that provided essential reagents, Marisi Castañón for help with baculovirus expression, Susanne Bloch and Clemens Gaumannmüller for their contributions during their rotations, and the Warren lab for helpful advice. This work was supported by the Austrian Science Fund by grant P21550-B12 to G.W. and C.L.dG.

REFERENCES

Araki Y, Gombos L, Migueleti SPS, Sivashanmugam L, Antony C, Schiebel E (2010). N-terminal regions of Mps1 kinase determine functional bifurcation. J Cell Biol 189, 41–56.

Bangs JD (2011). Replication of the ERES:Golgi junction in bloodstream-form African trypanosomes. Mol Microbiol 82, 1433–1443.

Barr FA, Silljé HHW, Nigg EA (2004). Polo-like kinases and the orchestration of cell division. Nat Rev Mol Cell Biol 5, 429–440.

Bonhivers M, Nowacki S, Landrein N, Robinson DR (2008). Biogenesis of the trypanosome endo-exocytotic organelle is cytoskeleton mediated. PLoS Biol 6, e105.

de Graffenried CL, Ho HH, Warren G (2008). Polo-like kinase is required for Golgi and bilobe biogenesis in *Trypanosoma brucei*. J Cell Biol 181, 431–438.

Dou Z, von Schubert C, Körner R, Santamaria A, Elowe S, Nigg EA (2011). Quantitative mass spectrometry analysis reveals similar substrate consensus motif for human Mps1 kinase and Plk1. PLoS One 6, e18793.

Elia AEH, Cantley LC, Yaffe MB (2003). Proteomic screen finds pSer/pThr-binding domain localizing Plk1 to mitotic substrates. Science 299, 1228–1231.

Esson HJ, Morriswood B, Yavuz S, Vidilaseris K, Dong G, Warren G (2012). Morphology of the trypanosome bilobe, a novel cytoskeletal structure. Eukaryotic Cell 11, 761–772.

Estévez AM, Kierszenbaum F, Wirtz E, Bringaud F, Grunstein J, Simpson L (1999). Knockout of the glutamate dehydrogenase gene in bloodstream Trypanosoma brucei in culture has no effect on editing of mitochondrial mRNAs. Mol Biochem Parasitol 100, 5–17.

Field MC, Carrington M (2009). The trypanosome flagellar pocket. Nat Rev Microbiol 7, 775–786.
Friedberg F (2006). Centrin isoforms in mammals. Relation to calmodulin. Mol Biol Rep 33, 243–252.
Gadelha C, Rothery S, Morphew M, McIntosh JR, Severs NJ, Gull K (2009). Membrane domains and flagellar pocket boundaries are influenced by the cytoskeleton in African trypanosomes. Proc Natl Acad Sci USA 106, 17425–17430.
Gheiratmand L, Brasseur A, Zhou Q, He CY (2013). Biochemical characterization of the bi-lobe reveals a continuous structural network linking the bi-lobe to other single-copied organelles in *Trypanosoma brucei*. J Biol Chem 288, 3489–3499.
Gull K (1999). The cytoskeleton of trypanosomatid parasites. Annu Rev Microbiol 53, 629–655.
Hammarton TC, Kramer S, Tetley L, Boshart M, Mottram JC (2007). *Trypanosoma brucei* Polo-like kinase is essential for basal body duplication, kDNA segregation and cytokinesis. Mol Microbiol 65, 1229–1248.
He CY, Pypaert M, Warren G (2005). Golgi duplication in *Trypanosoma brucei* requires Centrin2. Science 310, 1196–1198.
Hill KL (2010). Parasites in motion: flagellum-driven cell motility in African trypanosomes. Curr Opin Microbiol 13, 459–465.
Ikeda KN, de Graffenried CL (2012). Polo-like kinase is necessary for flagellum inheritance in *Trypanosoma brucei*. J Cell Sci 125, 3173–3184.
Klotz C, Garreau de Loubresse N, Ruiz F, Beisson J (1997). Genetic evidence for a role of centrin-associated proteins in the organization and dynamics of the infraciliary lattice in *Paramecium*. Cell Motil Cytoskeleton 38, 172–186.
Kohl L, Robinson D, Bastin P (2003). Novel roles for the flagellum in cell morphogenesis and cytokinesis of trypanosomes. EMBO J 22, 5336–5346.
Kohl L, Sherwin T, Gull K (1999). Assembly of the paraflagellar rod and the flagellum attachment zone complex during the *Trypanosoma brucei* cell cycle. J Eukaryot Microbiol 46, 105–109.
Lacomble S, Vaughan S, Gadelha C, Morphew MK, Shaw MK, McIntosh JR, Gull K (2009). Three-dimensional cellular architecture of the flagellar pocket and associated cytoskeleton in trypanosomes revealed by electron microscope tomography. J Cell Sci 122, 1081–1090.
Lacomble S, Vaughan S, Gadelha C, Morphew MK, Shaw MK, McIntosh JR, Gull K (2010). Basal body movements orchestrate membrane organelle division and cell morphogenesis in *Trypanosoma brucei*. J Cell Sci 123, 2884–2891.
LaCount DJ, Barrett B, Donelson JE (2002). *Trypanosoma brucei* FLA1 is required for flagellum attachment and cytokinesis. J Biol Chem 277, 17580–17588.
Li S, Sandercock AM, Conduit P, Robinson CV, Williams RL, Kilmartin JV (2006). Structural role of Sfi1p-centrin filaments in budding yeast spindle pole body duplication. J Cell Biol 173, 867–877.
Li Z, Umeyama T, Li Z, Wang CC (2010). Polo-like kinase guides cytokinesis in Trypanosoma brucei through an indirect means. Eukaryot Cell 9, 705–716.
Lutz W, Lingle WL, McCormick D, Greenwood TM, Salisbury JL (2001). Phosphorylation of centrin during the cell cycle and its role in centriole separation preceding centrosome duplication. J Biol Chem 276, 20774–20780.
Martindale VE, Salisbury JL (1990). Phosphorylation of algal centrin is rapidly responsive to changes in the external milieu. J Cell Sci 96, 395–402.
Mazanek M, Mituloviae G, Herzog F, Stingl C, Hutchins JRA, Peters J-M, Mechtler K (2007). Titanium dioxide as a chemo-affinity solid phase in offline phosphopeptide chromatography prior to HPLC-MS/MS analysis. Nat Protoc 2, 1059–1069.
Mok J *et al*. (2010). Deciphering protein kinase specificity through large-scale analysis of yeast phosphorylation site motifs. Sci Signal 3, ra12.
Morriswood B *et al*. (2013). Novel bilobe components in *Trypanosoma brucei* identified using proximity-dependent biotinylation. Eukaryot Cell 12, 356–367.
Morriswood B, He CY, Sealey-Cardona M, Yelinek J, Pypaert M, Warren G (2009). The bilobe structure of *Trypanosoma brucei* contains a MORN-repeat protein. Mol Biochem Parasitol 167, 95–103.
Nett IRE, Davidson L, Lamont D, Ferguson MAJ (2009a). Identification and specific localization of tyrosine-phosphorylated proteins in *Trypanosoma brucei*. Eukaryot Cell 8, 617–626.
Nett IRE, Martin DMA, Miranda-Saavedra D, Lamont D, Barber JD, Mehlert A, Ferguson MAJ (2009b). The phosphoproteome of bloodstream form *Trypanosoma brucei*, causative agent of African sleeping sickness. Mol Cell Proteomics 8, 1527–1538.
Portman N, Gull K (2012). Proteomics and the *Trypanosoma brucei* cytoskeleton: advances and opportunities. Parasitology 139, 1168–1177.
Robinson DR, Gull K (1991). Basal body movements as a mechanism for mitochondrial genome segregation in the trypanosome cell cycle. Nature 352, 731–733.
Robinson DR, Sherwin T, Ploubidou A, Byard EH, Gull K (1995). Microtubule polarity and dynamics in the control of organelle positioning, segregation, and cytokinesis in the trypanosome cell cycle. J Cell Biol 128, 1163–1172.
Salisbury JL (1995). Centrin, centrosomes, and mitotic spindle poles. Curr Opin Cell Biol 7, 39–45.
Salisbury JL, Baron A, Surek B, Melkonian M (1984). Striated flagellar roots: isolation and partial characterization of a calcium-modulated contractile organelle. J Cell Biol 99, 962–970.
Sanders MA, Salisbury JL (1994). Centrin plays an essential role in microtubule severing during flagellar excision in *Chlamydomonas reinhardtii*. J Cell Biol 124, 795–805.
Selvapandiyan A, Duncan R, Debrabant A, Bertholet S, Sreenivas G, Negi NS, Salotra P, Nakhasi HL (2001). Expression of a mutant form of *Leishmania donovani* centrin reduces the growth of the parasite. J Biol Chem 276, 43253–43261.
Selvapandiyan A, Kumar P, Morris JC, Salisbury JL, Wang CC, Nakhasi HL (2007). Centrin1 is required for organelle segregation and cytokinesis in *Trypanosoma brucei*. Mol Biol Cell 18, 3290–3301.
Sheehan JH, Bunick CG, Hu H, Fagan PA, Meyn SM, Chazin WJ (2006). Structure of the N-terminal calcium sensor domain of centrin reveals the biochemical basis for domain-specific function. J Biol Chem 281, 2876–2881.
Sherwin T, Gull K (1989). The cell division cycle of Trypanosoma brucei brucei: timing of event markers and cytoskeletal modulations. Philos Trans R Soc Lond B Biol Sci 323, 573–588.
Shi J, Franklin JB, Yelinek JT, Ebersberger I, Warren G, He CY (2008). Centrin4 coordinates cell and nuclear division in *T. brucei*. J Cell Sci 121, 3062–3070.
Szöör B (2010). Trypanosomatid protein phosphatases. Mol Biochem Parasitol 173, 53–63.
Szöör B, Wilson J, McElhinney H, Tabernero L, Matthews KR (2006). Protein tyrosine phosphatase TbPTP1: a molecular switch controlling life cycle differentiation in trypanosomes. J Cell Biol 175, 293–303.
Thingholm TE, Jørgensen TJD, Jensen ON, Larsen MR (2006). Highly selective enrichment of phosphorylated peptides using titanium dioxide. Nat Protoc 1, 1929–1935.
Thompson JR, Ryan ZC, Salisbury JL, Kumar R (2006). The structure of the human centrin 2-xeroderma pigmentosum group C protein complex. J Biol Chem 281, 18746–18752.
Trojan P, Rausch S, Giessl A, Klemm C, Krause E, Pulvermüller A, Wolfrum U (2008). Light-dependent CK2-mediated phosphorylation of centrins regulates complex formation with visual G-protein. Biochim Biophys Acta 1783, 1248–1260.
Vaughan S (2010). Assembly of the flagellum and its role in cell morphogenesis in *Trypanosoma brucei*. Curr Opin Microbiol 13, 453–458.
Vaughan S, Kohl L, Ngai I, Wheeler RJ, Gull K (2008). A repetitive protein essential for the flagellum attachment zone filament structure and function in *Trypanosoma brucei*. Protist 159, 127–136.
Vickerman K (1969). On the surface coat and flagellar adhesion in trypanosomes. J Cell Sci 5, 163–193.
Wang M, Gheiratmand L, He CY (2012). An interplay between Centrin2 and Centrin4 on the bi-lobed structure in *Trypanosoma brucei*. Mol Microbiol 83, 1153–1161.
Wirtz E, Leal S, Ochatt C, Cross GA (1999). A tightly regulated inducible expression system for conditional gene knock-outs and dominant-negative genetics in *Trypanosoma brucei*. Mol Biochem Parasitol 99, 89–101.
Yang A, Miron S, Duchambon P, Assairi L, Blouquit Y, Craescu CT (2006). The N-terminal domain of human centrin 2 has a closed structure, binds calcium with a very low affinity, and plays a role in the protein self-assembly. Biochemistry 45, 880–889.
Yang C-H, Kasbek C, Majumder S, Yusof AM, Fisk HA (2010). Mps1 phosphorylation sites regulate the function of centrin 2 in centriole assembly. Mol Biol Cell 21, 4361–4372.
Yu Z, Liu Y, Li Z (2012). Structure-function relationship of the Polo-like kinase in *Trypanosoma brucei*. J Cell Sci 125, 1519–1530.